

UNIVERSITÀ DEGLI STUDI DI PAVIA

---

FACOLTÀ DI INGEGNERIA

CORSO DI LAUREA MAGISTRALE IN INGEGNERIA BIOMEDICA

DIPARTIMENTO DI MECCANICA STRUTTURALE



# One Way and Two Way–Shape Memory Effect: Thermo–Mechanical Characterization of Ni–Ti wires

*Relatore*

Ch.mo Prof. Ferdinando Auricchio  
.....

*Correlatore*

Ch.mo Prof. Vincenzo Massarotti  
.....

*Laureanda*

Eleonora Zanaboni

---

ANNO ACCADEMICO 2007/2008

*Dedicate to my family  
and my aunt Franca*

# Abstract

Shape Memory Alloys (SMAs) have been considered as one of the most promising smart materials. They can provide novel solution in several fields, for various applications (e.g. actuator, biomedical application, clamping systems, ect.). Shape Memory Alloys demonstrate a unique ability to recover their initial shape after deformation through a reversible thermo-elastic phase transformation, it allows Shape Memory Alloys to recover large strains, either spontaneously (pseudoelasticity) or through an increase in temperature (Shape Memory Effect). Among the commercially available Shape Memory Alloys, nickel-titanium (Ni-Ti and Ni-Ti based) ones are outstanding due to their excellent performance and reliability, in addition to strain recovery, Ni-Ti is attractive for several medical applications due to its biocompatibility, corrosion resistance and fatigue behaviour.

Much of the prior work has concentrate on the link between microstructure and thermally induced phase, without examining the effect of different heat treatments on mechanical behavior, even though the microstructure and resulting thermo-mechanical properties are quite sensitive to heat treatment. The present study aims to provide a more comprehensive and fundamental link between structural and various behavioral changes in NiTi in response to heat treatment. In particular, a more precise study on the thermo-mechanical characterization of near equiatomic Ni-Ti wires to understand the mechanism and to value the performance in One Way Shape Memory Effect and Two Way Shape Memory Effect. Therefore, a series of tests has been programmed in laboratory in order to characterize the behavior of the Ni-Ti material with the aim to realize a device answering to the plan characteristics.

In order to achieve such a purpose, a systematic study employing Scanning Electron Microscopy (SEM), X-ray Diffraction (XRD), Differential Scanning Calorimeter (DSC) was carried out.

## ACKNOWLEDGEMENTS

First of all I would like to thank my supervisor Professor Ferdinando Auricchio for giving me the opportunity to work in the very interesting area of Shape Memory Alloys. In particular, I would thank him for sharing his ideas and knowledges with me, and helping me in all ways. I would also like to thank Professor Vincenzo Massarotti and Professor Doretta Capsoni, Doct. Stefania Ferrari and Doct. Corrado Tomasi in Department of Physical Chemistry, thanks in order to have to me followed out and to have allowed I use it of the equipments of the department laboratory.

I would also like to specially thanks Giuseppe Spinozzi for his valuable advice during my experimental times and for assisting me in experimental phase of my Dissertation. I would like to thank Lab. Structural Mechanics, my fellow colleagues: Eng. Michele Conti, Eng. Simone Morganti, Eng. Giuseppe Balduzzi and Doc. Laura Pozzi.

I would like to thank all my friends Alessandro, Barbara, Carla, Chiara and Isabella and I would like to special thank to Marilena, Ilaria, Mara, Giuliana, Vincenzo and Gill for amazing holidays spent together!!

I thank Billie Joe, Mike, Tré because they are always togheter with me.

I would like to also thank all my theachers of Ist.Magistrale 'A. Cairoli', they played a very important rule in my life.

I would like to also thank my family for being there for me throughout all the years I was a student.

In the end I do my deed!!

Thank you.

*It's something unpredictable, but in the end is right.*

*I hope you had the time of your life.*

# Contents

<b>Abstract</b>	<b>i</b>
<b>1 Introduction</b>	<b>6</b>
1.1 Introduction and scope of research . . . . .	6
1.2 History of shape Memory Alloys . . . . .	8
1.3 Fabrication of Ti-Ni based Alloys . . . . .	9
1.4 Medical applications of Shape Memory Alloys . . . . .	12
1.4.1 Biocompatibility of Ni-Ti Shape Memory Alloys . . . . .	12
1.4.2 Cardiovascular Applications . . . . .	13
1.4.3 Orthopedic Applications . . . . .	15
1.4.4 Surgical Instruments . . . . .	16
<b>2 Nickel-Titanium Shape Memory Alloys</b>	<b>18</b>
2.1 Phase Diagram of Ni-Ti Alloy System . . . . .	18
2.2 A Microscopic Perspective of Martensite . . . . .	20
2.3 Thermoelastic Martensitic Transformation . . . . .	22
2.4 Temperature Transformation in Shape Memory Alloys . . . . .	26
2.4.1 Measuring Transformation Temperatures in Ni-Ti Alloys	27
2.4.2 Hysteresis . . . . .	30
2.5 Mechanical and Functional Properties of Ni-Ti Alloys . . . . .	31
2.5.1 The Origin of Shape Memory Effect . . . . .	32
2.5.2 Shape Memory Effect (SME) . . . . .	34
2.5.3 Superelastic Effect (SE) . . . . .	37

<b>3</b>	<b>Characterization of SM Behaviour in Ni–Ti Alloys</b>	<b>41</b>
3.1	Summery of the Functional Properties . . . . .	41
3.1.1	Modelling the Shape Memory Behavior . . . . .	42
3.1.2	Thermodynamic Contribution of Defects . . . . .	42
3.2	Equipments . . . . .	43
3.3	Characterization of Ni–Ti alloy . . . . .	47
3.4	Differential Scanning Calorimeter Analysis . . . . .	49
3.4.1	Setting Conditions for Analysis . . . . .	53
3.5	DSC Results . . . . .	53
3.6	X-Ray Diffraction . . . . .	56
3.6.1	XRD Analysis . . . . .	58
3.7	Conclusion . . . . .	58
<b>4</b>	<b>Characterization of TWSM Behaviour in Ni–Ti Alloys</b>	<b>64</b>
4.1	Some Aspects of the Two Way Shape Memory Effect . . . . .	64
4.2	TWSM Training Processes . . . . .	66
4.2.1	TWSME Training by Overdeformation . . . . .	66
4.2.2	Training by Shape Memory Cycling . . . . .	67
4.2.3	Training by Pseudoelastic (PE) Cycling . . . . .	67
4.2.4	Training by Combined SME/PE Training . . . . .	67
4.2.5	Constrained Temperature Cycling of DM . . . . .	68
4.3	Degradation of the Shape Memory Effect . . . . .	68
4.4	Experiment . . . . .	70
4.5	Results and Discussion . . . . .	73
4.6	Conclusions . . . . .	74
<b>5</b>	<b>Conclusion and Future Developements</b>	<b>78</b>
	<b>Bibliografia</b>	<b>i</b>

# List of Figures

1.1	Device for Minimally Invasive Surgery (MIS) . . . . .	8
1.2	Fabbrication processes of Ni–Ti . . . . .	9
1.3	Forming . . . . .	11
1.4	Cardiovascular Applications . . . . .	14
1.5	Ortophedic Applications . . . . .	15
1.6	Some kinds of Endoscopy . . . . .	16
1.7	Fabbrication processes of Ni–Ti . . . . .	17
2.1	Phase diagram of Ni–Ti alloy . . . . .	19
2.2	Austenite and Martensite Crystallography . . . . .	21
2.3	Two transformation paths in Ti-Ni alloys . . . . .	22
2.4	Martensitic trasformation (MT) . . . . .	23
2.5	Slip and Twinning Accomodate Mechanism . . . . .	24
2.6	Twin Boundary plain . . . . .	25
2.7	Slip and Twinning Accomodate Mechanism . . . . .	25
2.8	Phase Transformation Temperatures of SMA material . . . . .	27
2.9	Costant Load Test . . . . .	28
2.10	Differential Scanning Calorimeter . . . . .	29
2.11	Active Af Test . . . . .	30
2.12	Hysteresis . . . . .	31
2.13	Stress–Strain–Temperature Curve . . . . .	33
2.14	Mechanism of Shape Memory Effect . . . . .	34
2.15	Schematically Origin of Shape Memory Effect . . . . .	35
2.16	Macroscopically Mechanism of One Way Shape Memory Effect	36
2.17	Macroscopically Mechanism of Two Way Shape Memory Effect	37

2.18	Superelastic Effect of a Ni–Ti SMA . . . . .	38
2.19	Schematic Diagram representing SME–SE . . . . .	39
3.1	RO tube furnace and controller . . . . .	44
3.2	Trendicator 400a Digital Temperature Display . . . . .	44
3.3	34411A Digital Multimeter . . . . .	45
3.4	Scanning Electron Microscope (SEM) . . . . .	45
3.5	Differential Scanning Calorimetry DSC . . . . .	46
3.6	Konus microscope #5424 . . . . .	47
3.7	Schematization Ni–Ti fixed on stainless steel bar . . . . .	49
3.8	Surface morfology of the wire . . . . .	50
3.9	Ni–Ti wires heat–treatment . . . . .	52
3.10	Schematization of DSC analysis machine . . . . .	52
3.11	DSC thermogram of a Ni–Ti alloy . . . . .	55
3.12	DSC thermogram of a Ni–Ti alloy . . . . .	57
3.13	XRD spectrum of a Ni–Ti alloy . . . . .	59
3.14	XRD spectrum of a Ni–Ti alloy . . . . .	60
3.15	XRD spectrum of a Ni–Ti alloy . . . . .	61
3.16	XRD spectrum of a Ni–Ti alloy . . . . .	62
3.17	Ni–Ti wires heat–treatment . . . . .	63
4.1	Different Training Procedures . . . . .	69
4.2	Schematization of the wire profile . . . . .	71
4.3	Schematization of procedure used to obtain TWSME . . . . .	72
4.4	Schematization of procedure used to obtain TWSME . . . . .	76
4.5	Comparison the TWSME obtain with two different training procedures	77

# List of Tables

2.1	Ni–Ti mechanical properties . . . . .	20
2.2	Comparison of Nitinol with that of stainless steel . . . . .	20
2.3	Summary of Ni–Ti technical specifications . . . . .	40
3.1	Specifications . . . . .	46
3.2	Commercial codes of Ni–Ti types . . . . .	48
3.3	Labeling and heat-treatment of specimens . . . . .	51
3.4	DSC samples analyzed . . . . .	53

# Chapter 1

## Introduction

### 1.1 Introduction and scope of research

In this dissertation, the results of the research activities carried out during the experimental period at the University of Pavia are presented. The aim of these activities regarded the interesting field of smart materials and, in particular, some aspects related to the functional behaviour of nickel–titanium (Ni–Ti) Shape Memory Alloys (SMAs).

Smart materials are able to note an external stimulus responding in a predetermined and repeatable manner; this capacity permits to interact with the material changing its geometrical and thermomechanical conditions. In this field, SMAs are a class of materials able to remember a predetermined configuration and to recover it as consequence of thermal or mechanical loads [4].

Shape memory alloys are known for their excellent memory phenomena accompanied with practical applicability. The special functional properties of SMAs are Shape Memory Effect (SME) and Superelastic Effect (SE).

Shape memory alloys may have two different kinds of Shape Memory Effect, these are common known as one-way shape memory effect (OWSME) and two-way shape memory effect (TWSME).

The Shape Memory Effect (SME) changes with temperature variation are mainly attributed to martensitic phase transformation. Usually these alloys

show two transformation phases: austenitic (parent phase B2 cubic) at high temperature and martensitic (B19' monoclinic phase) at low temperature [6], [50]. Thermoelastic martensitic transformation is very sensitive to thermal cycling; Humbeeck et al. [18] observed that several mechanisms are active during thermal cycling such as introduction of defects and accommodation of stresses at the grain boundaries. The transformation process gets stabilized due to the irreversible changes in the microscopic state introduced during thermal cycling. It can be characterised by measuring structure sensitive properties such as the electrical resistivity [46].

Near equiatomic Ni–Ti alloys are the most promising Shape Memory Alloys in terms of practical applicability. In fact, in addition to austenite-martensite phase transformation, there is another intermediate phase known as the ‘R-phase transformation’ where, upon lowering the temperature, the austenite cubic structure can distort gradually to a rhombohedral lattice structure. This R-phase is a function of heat treatment temperature, thermal and mechanical cycles [9]. For this reason, a systematic study to promote the R-phase as a function of heat treatment temperature is developed in this dissertation. In fact, the R-phase transformation is important for an actuator Ni–Ti wire (as explained followed). Another important aspects of NiTi alloys are related to the biocompatibility, superior mechanical and corrosion properties, which have allowed the greater use and employment in biomedical field.

In this dissertation, the results related to different investigations carried out on a Ni–Ti alloy wire are presented. In particular, the thermomechanical behaviour of the material was investigated to better understand the mechanisms involved in the shape memory effect, using proper experimental procedures. First of all, the Ni–Ti wires were due to thermo-mechanical characterized in One Way Shape Memory Alloys and then, the thermal cycling given to the heat-treated on Ni–Ti wire samples were investigated by a series of Differential Scanning calorimeter (DSC) and X-ray Diffraction (XRD). Finally, the Ni–Ti wires were trained with different thermo-mechanical processes for obtain Two Way Shape Memory Alloys and their properties were

examined for future scopes in biomedical field. In particular, this work casts the bases for research in the development on the tips for the endoscopic devices in MIS (Minimally Invasive Surgery) to be moved by Two Way Shape Memory Effect Ni-Ti (Fig. 1.1).

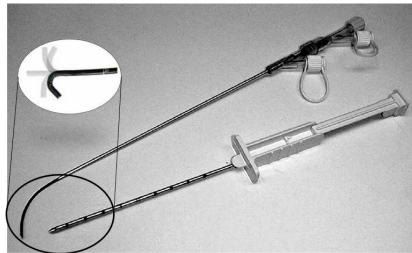


**Fig. 1.1:** Device for Minimally Invasive Surgery (MIS): Flexible and Rigid Endoscopies for Gastroscopy, with the tip particular.

## 1.2 History of shape Memory Alloys

The first reported steps towards the discovery of the Shape Memory Effect were taken in the 1930s, when A. Ölander discovered the pseudoelastic behaviour of the Au-Cd alloy in 1932. Greninger and Mooradian (1938) observed the formation and disappearance of a martensitic phase by decreasing and increasing the temperature of a Cu-Zn alloy. The basic phenomenon of the memory effect governed by the thermoelastic behaviour of the martensite phase was widely reported a decade later by Kurdjumov and Khandros (1949) and also by Chang and Read (1951).

In the early 1960s, Buehler and his co-workers at the U.S. Naval Ordnance Laboratory discovered the Shape Memory Effect in an equiatomic alloy of nickel and titanium, which can be considered a breakthrough in the field of shape memory materials. This alloy was named Nitinol (Nickel-Titanium Naval Ordnance Laboratory). The use of NiTi as is fascinating because of its special functional behaviour, which is completely new compared to the conventional metal alloys.

## 1.3 Fabrication of Ti-Ni based Alloys

The Ni-Ti alloy is an equiatomic intermetallic compound and a composition shift from stoichiometry affects the characteristics of the alloy. In par-

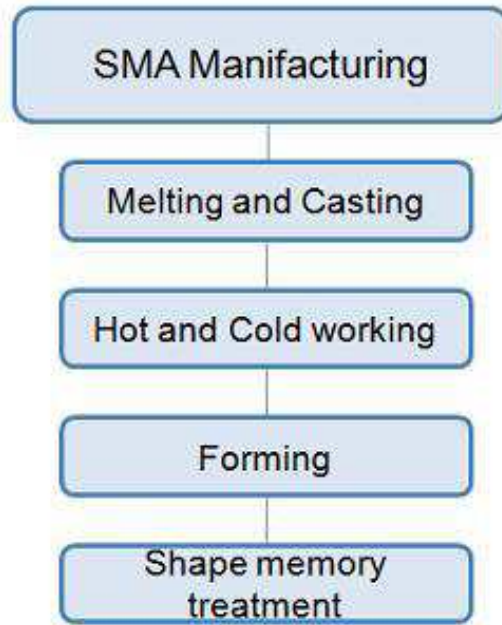


**Fig. 1.2:** Fabbriation processes shows a typical fabbriation processes of Ni–Ti shape memory alloy.

ticular, trasformation temperatures are extremely sensitive to composition. Therefore, some problems exist in the fabrication of commercial SMA (Ni–Ti SMA): control of the chemical alloy composition, cold and hot-working and shape memory treatment (heat-treatment).

In this section, fundamental fabrication processes of Ni-Ti based alloys (Fig. 1.2) are brief presented.

1. **Melting and casting processes:** is the first step in Ti-Ni alloy fabrication. The common melting method used is in high vacuum or an inert gas atmosphere [39]. In particular, a high frequency induction melting method is most commonly used. Moreover, the first advantage of induction melting is the homogeneity of chemical composition

throughout the ingot, another advantage of induction melting is the controllability of chemical composition.

Electron beam melting, argon arc melting and plasma arc melting are also employed.

- Electron beam melting utilizes a high-voltage electron beam as the heating source;
- Argon arc melting utilizes a non-consumable electrode or a consumable electrode consisting of materials to be melted;
- Plasma arc melting utilized a low velocity electron beam discharged from a hollow plasma cathode.

2. **Hot- and Cold-working processes:** are applied to reach the desired dimensions, the ingot is forged and rolled into a bar or a slab with appropriate size. Rod or wire products are roll-worked using a bar rolling mill.

Compared to the hot-working, cold-working of Ni-Ti alloy is more difficult. The workability strongly depends on the chemical alloy composition. It becomes harder with increasing Ni content. In particular, working becomes difficult when the Ni content is more than 51 at % . The optimum heating temperature for hot-working and to reach the final dimensions of the Ni-Ti, which part should pass through several reduction stages, is around 600-800 °C .

To carry out a satisfactory working, an optimal setting which combines the drawing and annealing processes has to be planned. Adhesion of wire to tools often occurs lubricants, sodium stearate soap, graphite-containing water based and oil based lubricant are employed.

3. **Forming:** most cold-drawing SMA wires are finally shaped by forming. A small number of springs are prepared by a method in which the Ni-Ti wire is wound on cylindrical jig. In commercial production, the coil spring are formed with use of an automatic forming machine, Fig. 1.3 shows the forming process of the helical coil schematically. The forming

process may be complex depending on the nature of the application and the parts may have to go through a multi-stage process to attain their final shapes.

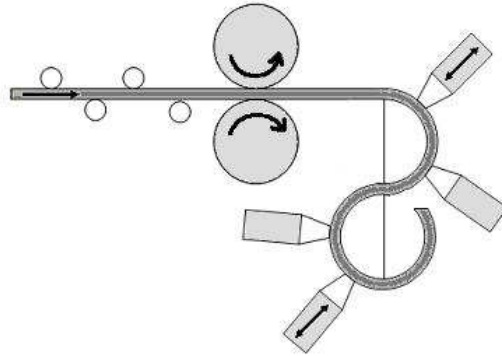


**Fig. 1.3:** Forming: Operating principal of the coil forming machine.

- 4. Shape memory treatment:** is the final process of Ti-Ni SMA fabrication. The most used treatment is the so-call ‘medium temperature treatment’ [?]. A range of 350-450 °C has been found to be a suitable heat-treating range for Ni-Ti, the formed Ni-Ti parts need to be fastened on a jig during heating to ensure. The holding time ranges from 10 to 100 min depending on the product size. The heat-treatment temperature is adjusted to achieve optimized properties in according to product specification.

In addition to the medium temperature treatment, several other methods of shape memory treatments have been used. But, the medium temperature treatment is mostly used as reveal superelasticity as reveal Shape Memory Effect in particular, One Way Shape Memory Effect (OWSME). Instead, the aging treatment, common known as ‘training process’, is often used to improve Two Way Shape Memory Effect (TWSME).

## **1.4 Medical applications of Shape Memory Alloys**

As seen mostly above, in view of SMA peculiar features and functional properties, SMAs are employed in various fields, for example in sensors/actuators, aerospace application, civil application and biomedical applications.

Biomedical Engineering is an interdisciplinary branch of engineering in which the principles and tools of traditional engineering fields, such as mechanical, materials, electrical, computer and chemical engineering, are applied to biomedical problems. Therefore, the main objectives of Biomedical Engineering are design, development and proper use of materials, devices, apparatus, equipment and techniques for diagnosis, treatment and rehabilitation of the patients, among these, the Shape Memory Alloys have a well-defined applicability.

Applications of SMA in the biomedical field have been successful for their functional properties, they are enhancing the possibility and the execution of less invasive surgeries. The biocompatibility of these alloys are one of their most important features as discussed better in next subsection.

Different applications exploit the Shape Memory Effect (mostly One Way Shape Memory effect) and the pseudoelasticity, so that they can be employed in orthopedic and cardiovascular applications and many others biomedical fields.

The following subsections presented a discussion of the biocompatibility Ni–Ti alloys and the biomedical applications of SMA; in particular, cardiovascular applications and orthopedic applications (two biomedical fields in which Nitinol-SMA have been employed extensively and successfully) and surgical applications.

### **1.4.1 Biocompatibility of Ni–Ti Shape Memory Alloys**

Biocompatibility is the ability of a material to remain biologically innocuous during its functional period inside a living body [26]. The period during which a biomaterial remains inside the human body is an important aspect

to be considered concerning its use, this is a crucial factor for the use of SMA devices in the human body.

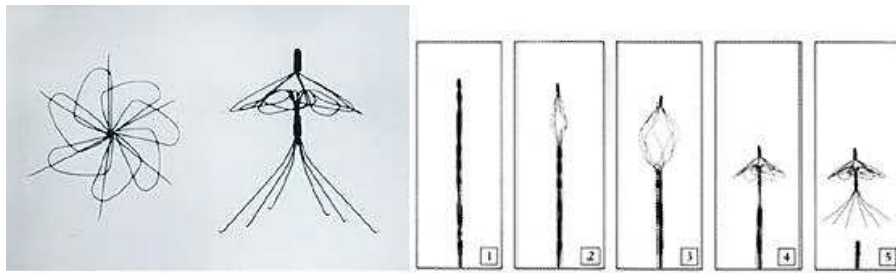
Several investigations have been conducted in order to establish the biocompatibility of Ni–Ti–based alloys and involved in medical applications. In fact, nickel–titanium and its compounds are biocompatible. In addition to that, the oxidation reaction of titanium produces an innocuous layer of  $\text{TiO}_2$  which surrounds the sample. This layer is responsible for the high resistance to corrosion of titanium alloys, and the fact that they are harmless to the human body. Due to the biocompatibility of the Nitinol and the high mechanical performances, there are a lot of possibilities to develop improved and innovative products applied successfully in biomedical field.

### 1.4.2 Cardiovascular Applications

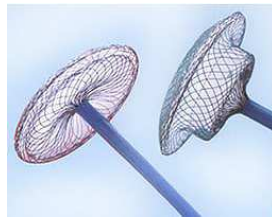
The first cardiovascular device developed with Shape Memory Alloys was the Simon filter [43]. The Simon filter (Fig. 1.4(a)) represented a new generation of devices, it is used for blood vessel interruption in order to prevent pulmonary embolism.

The atrial septal occlusion device (Fig. 1.4(b)) is an alternative to surgery. This device is composed of SMA wires and a water–proof film of polyurethane. As is the case for the Simon filter, the surgery to place this device exploits the Shape Memory Effect (SME), being much less invasive than the traditional one. First, one half of the device is inserted through a catheter by the vena cava up to the heart, in its closed form. Then, it is placed on the atrial hole and opened, recovering its original shape. Next, the second half of the device is placed by the same route as the first one, and then both halves are connected.

Stents are another one of the most important cardiovascular applications that are used to maintain the inner diameter of a blood vessel. Actually, these devices are used in several situations in order to support any tubular passage such as the esophagus and bile duct, and blood vessels such as the coronary, iliac, carotid, aorta and femoral arteries (Fig. 1.4(c)).



(a)



(b)



(c)

**Fig. 1.4:** Cardiovascular Application : (a) The Simon Filter shown in longitudinal and transverse views of the deployed state (left), steps of operation of Simon filter(right), (b) the Atrial Septal-Defect occlusion device is used to seal holes in the heart wall, (c) Shape memory self-expanding stents.

### 1.4.3 Orthopedic Applications

SMA's have had a large number of orthopedic applications. The spinal vertebra spacer (Fig. 1.5(a)) is one.

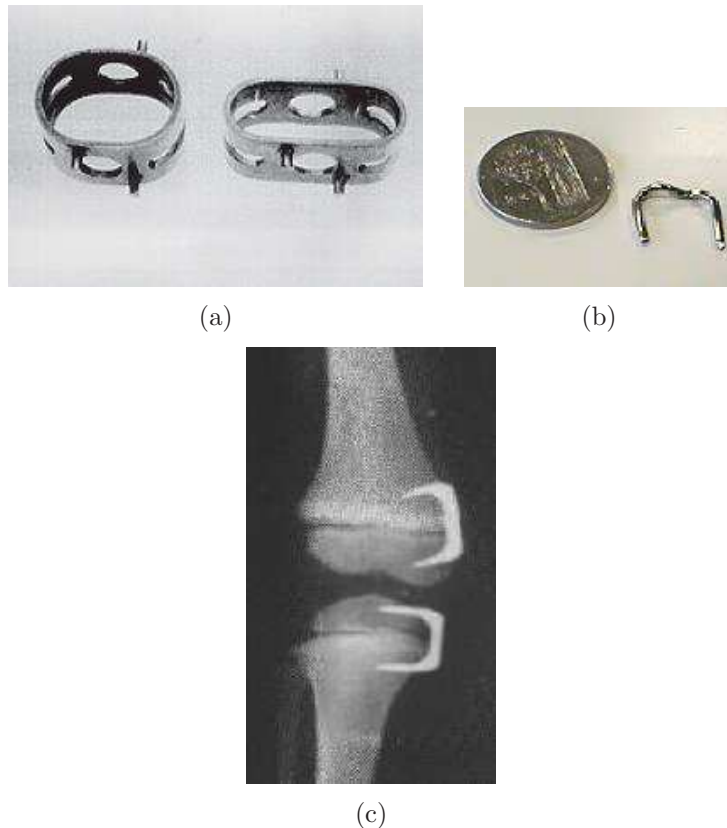


**Fig. 1.5:** Orthopedic Applications : (a) shape memory spacers in the martensitic state (left) and in the original shape (right), (b) orthopedic staples for human leg, (c) X-ray of a human foot.

The insertion of this spacer between two vertebrae assures the local reinforcement of the spine, preventing any traumatic motion during the healing process.

Another application in the orthopedic field is related to the healing process of broken and fractured bones. Several types of shape memory orthopedic staples (Fig. 1.5(b)) are used to accelerate the healing process of bone fractures, exploiting the Shape Memory Effect. (Fig. 1.5(c)) shown an application of these staples during the healing process of a patients leg

fracture.

#### 1.4.4 Surgical Instruments

Since medical researchers have made recent attempts to develop less invasive surgeries (Minimal Invasive Surgical), Shape Memory Alloys have been used to fabricate some surgical instruments.

In surgical endoscopic procedures, the very large amount of recoverable deformation is primarily the key characteristics sought in these types of applications. In the years, different kinds of endoscopic devices are developed: rigid endoscopy, flexible endoscopy, semirigid endoscopy. The flexibility of nitinol tubing has been used in orthopedic bone reamer application, arthroscopic guides, flexible protections for delicate optical or laser-delivery fibers, needles, biopsy devices, etc. Some of different types of endoscopies are shown in Fig. 1.6

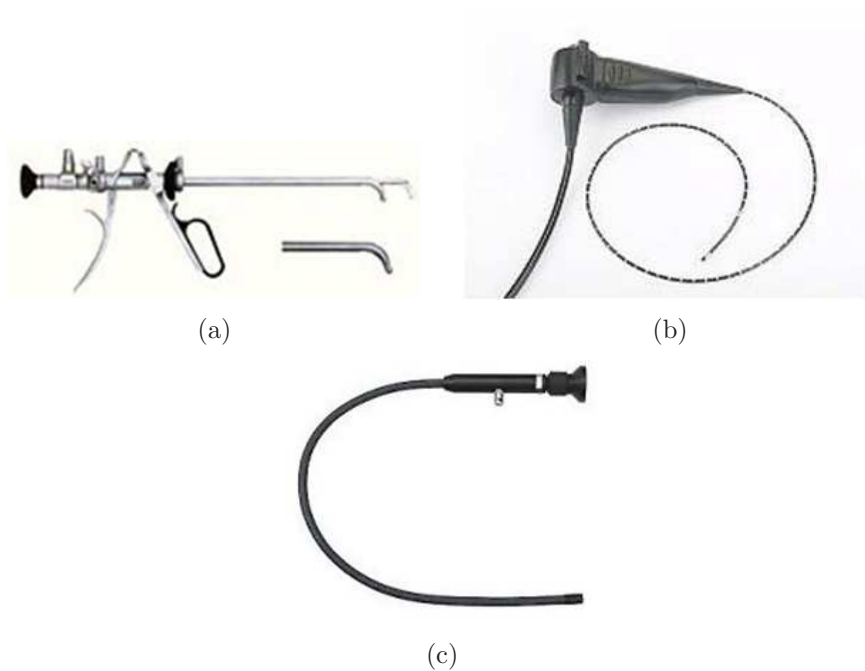


**Fig. 1.6:** Some kinds of Endoscopy: (a) Rigid endoscopy, (b) Flexible endoscopy, (c) Semi-flexible endoscopy.

The use of SMAs in laparoscopic surgical instruments has also been suc-

#### 1.4 Medical applications of Shape Memory Alloys

---

cessful. In Fig. 1.7 shows some SMA surgical tools. These devices allow smooth movements tending to mimic the continuous movement of muscles. These devices facilitate access to intricate regions.

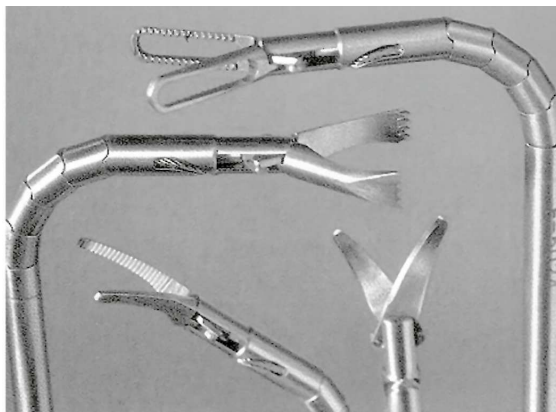


**Fig. 1.7:** Laparoscopy tools: the SMAs surgical tools such as grippers and scissors.

# Chapter 2

## Nickel–Titanium Shape Memory Alloys

In this chapter, the properties of Shape Memory Alloys (SMAs) are presented. We begin by looking at the physical characteristics at microscopic level, and move on to explain how the phase changes that we observe microscopically bring about the Shape Memory Effect (SME). Then, we explain the macroscopic behavior of SMAs and their properties.

NiTi alloys are the most promising Shape Memory Alloys in terms of practical applicability. Generally, the use of these alloys seems to be very useful in applications where it is necessary to use smart components with low dimensions, for this reason Ni–Ti alloys are becoming very interesting.

### 2.1 Phase Diagram of Ni–Ti Alloy System

Many investigations have been made on the equilibrium phase diagram of the Ni–Ti system. The phase diagram of Ti–Ni alloy system is important for heat-treatments of the alloys and improvement of the shape memory characteristics. Fig. 2.1 is a phase diagram of Ti–Ni alloy system by Massalski et al. [31]. The region of great interest is restricted in the central region bounded by  $\text{Ti}_2\text{Ni}$  and  $\text{TiNi}_3$  phases, since the single phase ‘Ti–Ni’ B2 transforms into a monoclinic phase martensitically B19’ (discussed in detail in the next sec-

## 2.1 Phase Diagram of Ni–Ti Alloy System

tion).

The main problems are the presence/absence of a eutectoid decomposition

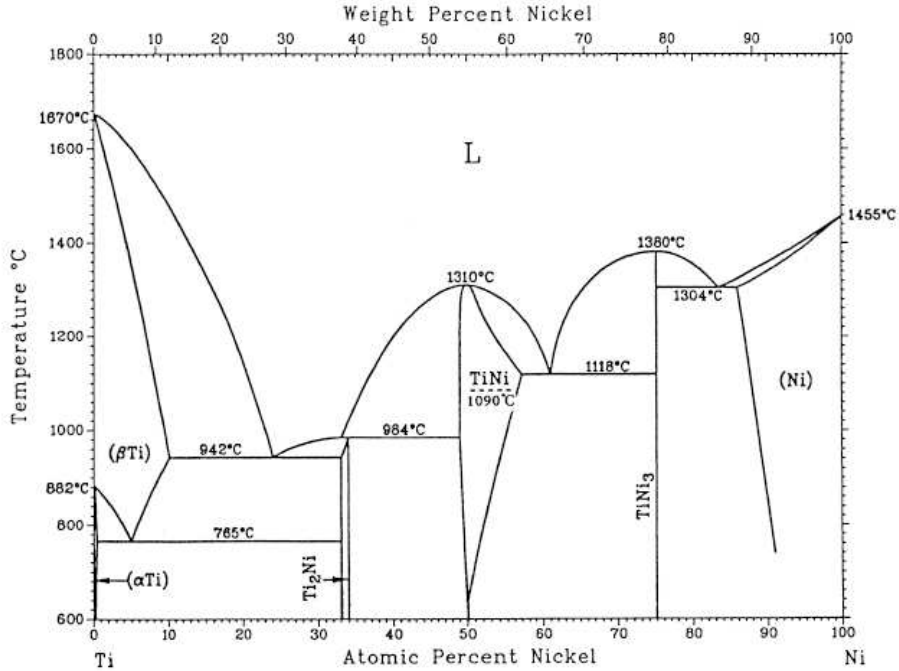
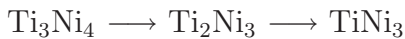


**Fig. 2.1:** Phase diagram of Ni–Ti alloy. A dotted line at 1090°C was added for order-disorder transition for Ni–Ti. See text for more details [31].

of  $\text{TiNi} \rightarrow \text{Ti}_2\text{Ni} + \text{TiNi}_3$  at 630°C, and the examination to the origin of  $\text{Ti}_3\text{Ni}_4$  and  $\text{Ti}_2\text{Ni}_3$  phases, which appear when Ti–Ni alloy is heat-treated under certain conditions. Anyhow, the presence of the eutectoid reaction was confirmed by detailed studies, which have put in evidence  $\text{Ti}_3\text{Ni}_4$  and  $\text{Ti}_2\text{Ni}_3$  are metastable phases and that the precipitation process occurs with ageing time until reaches a stable phase of  $\text{TiNi}_3$ .



A dotted line at 1090°C indicates BCC  $\rightarrow$  B2 transition, in this way, it is possible to consider heat-treatments using this phase diagram to improve shape memory characteristics. The crystal structures of  $\text{Ti}_3\text{Ni}_4$  and  $\text{Ti}_2\text{Ni}_3$  phases were determined also. In Fig. 2.1 is not possible to hold on the precipitation hardening by  $\text{Ti}_2\text{Ni}$  phase, seeing that the phase boundary of Ti–Ni phase on Ti-rich side is vertical and there is not alteration in solubility limit with lowering temperature.

## 2.2 A Microscopic Perspective of Martensite

Ni–Ti Shape Memory Alloys can exist in a two different temperature-dependent crystal structures called martensite phase (lower temperature) and austenite phase or parent phase (higher temperature). Typically mechanical properties of austenitic Ni–Ti are different to the same properties in martensitic NiTi, Tab. 2.1. For this reason, SMA in austenite and in martensite can be consider as two different materials. Besides, in Tab. 2.2 shows a summary of comparison of Ni–Ti with properties of stainless steel, for better understanding the greatest employment in various fields of SMAs.

	AUSTENITE	MARTENSITE
Youngs modulus	30–83 GPa	20–45 GPa
Ultimate Tensile Strength	800–1900 MPa	800–1900 MPa
Elongation at Failure	20–25%	20–25%
Recoverable strain	8–10 %	8–10%
Poisson Ratio	0.33	0.33

**Tab. 2.1:** Ni–Ti mechanical properties.

Property	NiTi	Stainless Steel
Recovered Elongation	8%	0.8%
Biocompatibility	Excellent	Fair
Torqueability	Excellent	Poor
Density	6.45 g/cm <sup>3</sup>	8.03 g/cm <sup>3</sup>
Magnetic	No	Yes
Resistively	80 to 100 micro–ohm*cm	72 micro–ohm*cm

**Tab. 2.2:** Comparison of Nitinol with that of stainless steel for more explanation see <http://web.archive.org/web/20030418012213> and insert the followed link : <http://www.sma-inc.com/NiTiProperties.html> .

However, the martensite crystal is produced from parent crystal without diffusion. Diffusionless transformations are those in which the new phase can only be formed by moving atoms random over relatively short distances

## 2.2 A Microscopic Perspective of Martensite

---

(where short distance means moving atoms are less than the interatomic distance).

The austenite is characterized by a Body Centered Cubic structure (BCC),

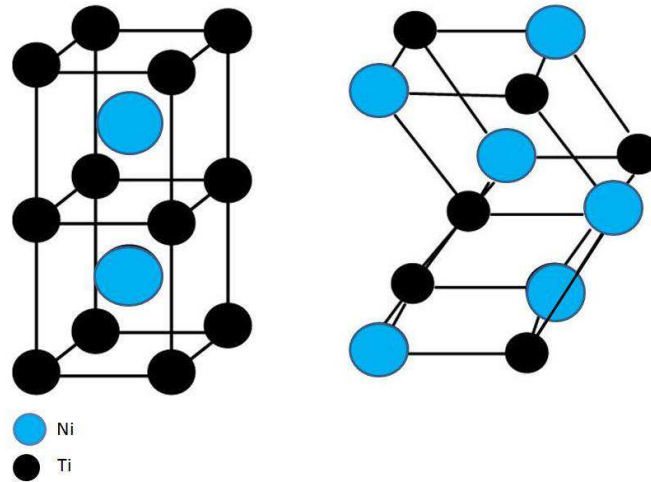


**Fig. 2.2:** Crystallography: (left) Austenite: austenitic phase (B2) is microstructurally ordered, (right) Martensite lattice structures: martensitic phase (B19') is less symmetric.

where there is a Nickel atom at the center of the crystallographic cube and a Titanium atom at each of the cubes eight corners, the austenitic phase is microstructurally symmetric. The ordered BCC structures are usually B2 type. This is the phase which plays an important role in the martensitic transformation and the associated shape memory effects. Typically, under solution-treated conditions, a near-equiatomic Ni–Ti alloys exhibit a transformation between a high temperature B2 phase, known also as the parent phase, and a low temperature B19' monoclinic phase, known as the martensite. The martensite phase of Ni–Ti is less symmetric and its lattice structure consists of a rhombus alignment with an atom at each of the rhombus corners. Fig. 2.2 shows two Ni–Ti crystals in the austenite (B2 phase) and martensite phases (B19').

However, under certain circumstance, such as cold working, thermal cycling, heat-treatment or chemical composition, an intermediate phase, known as rhombohedral phase or the R-phase, may appear between the austenite and the martensite, causing a two-stage transformation behavior as shown

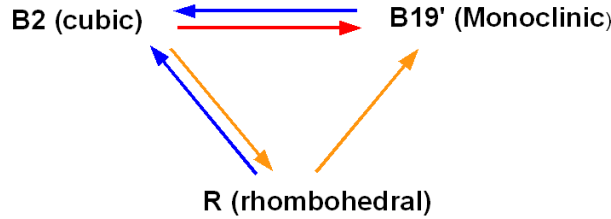


**Fig. 2.3:** Two transformation paths in TiNi alloys: one stage transformation phase  $B2 \rightarrow B19'$ , two stage transformation phase  $B2 \rightarrow R\text{-phase} \rightarrow B19'$ , reverse transformation:  $B19' \rightarrow B2$ ,  $R\text{-phase} \rightarrow B2$

in Fig. 2.3.

Bataillard et al. observed that the formation of the R-phase occurs in relation to stress fields surrounding coherent  $Ni_4Ti_3$  precipitates. Khalil-Allafi and co-workers investigated the effect of aging as a function of time and temperature, and they suggested that microstructural and chemical heterogeneity also play an important role in the phase transition sequence observed in multi-step transitions. Another way to stabilize the R-phase in binary Ni–Ti alloys is to introduce dislocations, usually by cold working. Only in ternary alloys such as NiTiFe, NiTiAl, or NiTiCo is the R-phase known to occur spontaneously. Thus, the structure determination of the R-phase in binary Ni–Ti is always a challenge because of the presence of other phases, defects, and texture are introduced [25][32][29]

## 2.3 Thermoelastic Martensitic Transformation

The unique behavior (SME and Superelasticity (SE)) of Ni–Ti is based on the temperature dependent austenite to martensite phase transformation on an atomic scale, which is commonly called Thermoelastic Martensitic Transformation (TMT)[33]. TMT starts by a shear like mechanism as shown in Fig. 2.4, different orientations in region A and B are called the correspondence variants of the martensites (since the martensite has a lower symmetry, many variants can be formed from the same parent phase). If the temperature is raised and the martensite becomes unstable, the reverse transformation

### 2.3 Thermoelastic Martensitic Transformation

---

(RT) occurs, and if the crystallographically reversible, the martensite reverts to the parent phase in the original orientation [33].

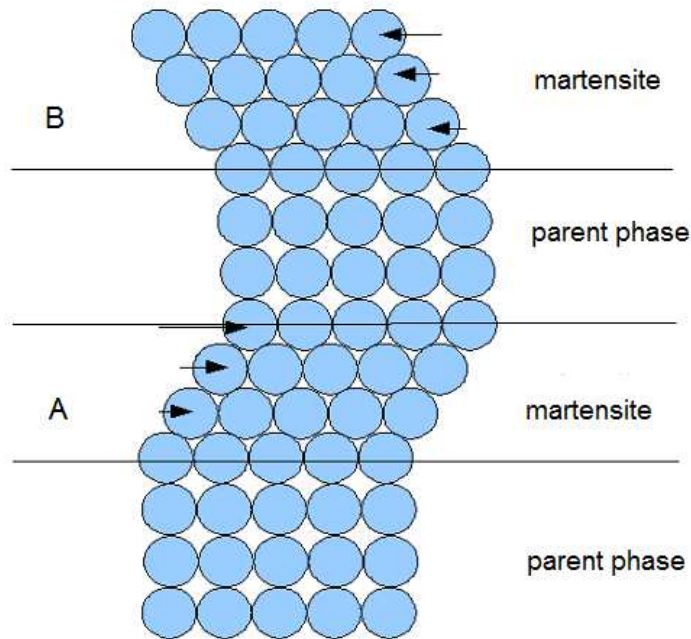


**Fig. 2.4:** Martensitic Transformation simple model.

In a crystallographic context, the phase transformation from austenite to martensite is thought of to occur in two mechanisms: *the Bain strain* and *the lattice invariant shear*. These mechanisms in a crystallographically are quite complex. However, they are possible to explain in a quite simple way using a two-dimensional approach. The Bain strain, namely also lattice deformation, consists on a series of atomic movements on small staircase (inferior to the distances between atoms) that it bring to the formation of a new phase. Thus, although the Bain strain is complicated, the combined effect of the Bain strain and lattice invariant shear is to convert the macroscopic strain into a shear.

In fact, martensite transformation (MT) is associated with a shape change combined with a large strain arises around the martensite when it is formed in austenite phase. To reduce the strain is important in the growth processes

of MT, the mechanism to obtain it is called lattice invariant shear (LIS). There are two possible LIS mechanisms : slip and twinning Fig. 2.5. Slip or twinning is a necessary process in martensite transformation, which of them is introduced depends upon the kinds of alloys, but twinning is usually introduced as a LIS in SMA [33].

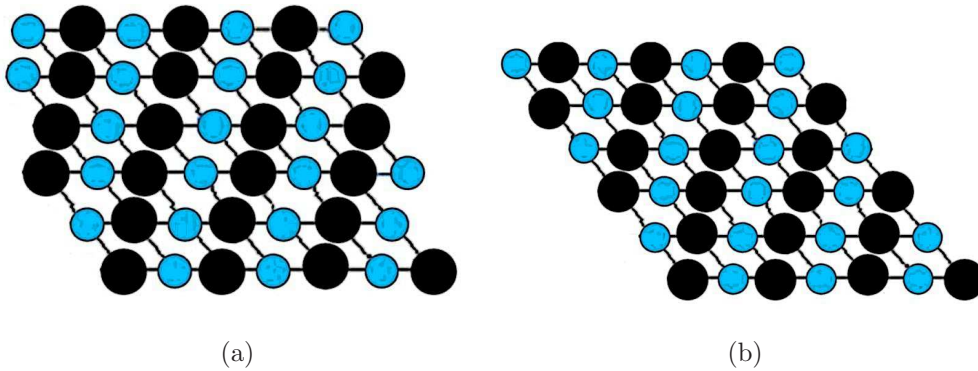


**Fig. 2.5:** Slip and Twinning Accommodate Mechanism in Martensite: (a) Slip accommodate mechanism of martensite (for example in steel), (b) Twinning mechanism in martensite SMA.

Thus, in twinning process, a twin is created by a proper shear, in particular, a two twin crystals are related by a symmetry operation with respect to a mirror plane, called twin boundary plain ( Fig. 2.6).

Crystal twinning occurs when two separate crystals share some of the same crystal lattice points in a symmetrical manner. The result is an intergrowth of two crystals in a variety of specific configurations separated by a twin boundary surface.

Twin boundaries occur when two crystals of the same type intergrowth, so that only a slight misorientation exists between them, the atoms situated on that twin boundary see the same number and type of bonds in both directions. Some key properties of twin boundaries plain are that they are of a very low energy and they are quite mobile; thus the relative stability of a martensitic phase is not strongly affected by the number or location of these boundaries.

The important different between slip and twinning is the first accommodation requires that atomic bonds be broken, while all bonds remain intact

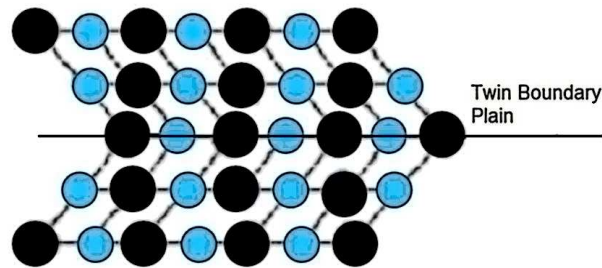


**Fig. 2.6:** Twin boundary plane: Twinned martensite.

in the twinned structure. In fact, if a stress is applied to the structure the twin boundaries will easily move, during this deformation, to produce a shape which better accommodates the applied stress. This results in a condensation of many twin variants to a single variant. This process is called detwinning shown in Fig. 2.7(c). Using a two-dimensional view, Fig. 2.7 shows that detwinned martensite structure [23]. Twinning and detwinning process are typically mechanisms used in SMA, these microscopically mechanisms are the basis for explain the macroscopic SMA properties.

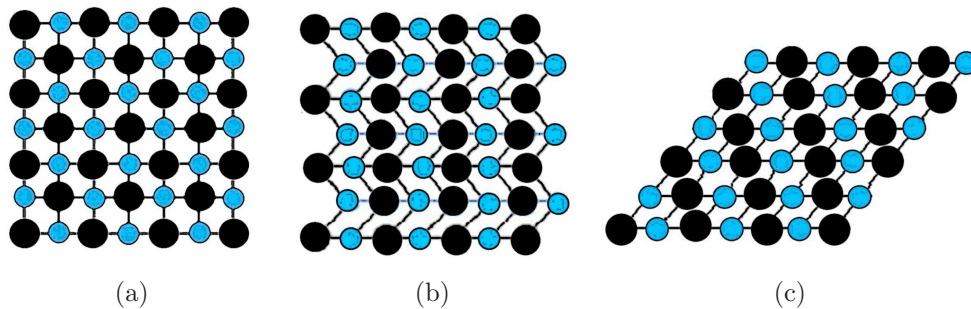


**Fig. 2.7:** Mechanism: Austenite and martensite microstructural view in a two-dimensional plan: (a) high temperature austenite cubic structure, (b) low temperature martensite twinned lattice structure, (c) martensite detwinning.

## 2.4 Temperature Transformation in Shape Memory Alloys

For almost any use of a Shape Memory Alloy, it is highly desirable to know the Transformation Temperatures (TTRs) of the alloy. The TTRs are those temperatures at which the alloy changes from the higher temperature Austenite to the lower temperature Martensite and viceversa.

SMA's do not undergo their phase transformation from martensite to austenite or from austenite to martensite at one specific temperature. The transformations begin at one temperature and stop at another. These start and finish temperatures are different depending on whether the material is heating or cooling. In order of lowest to highest temperature, they are defined:

- *Martensite finish ( $M_f$ )*: temperature at which the material is completely twinned martensite which does not entail a change in shape if unloaded
- *Martensite start ( $M_s$ )*: temperature at which, when austenite is cooled, it begins to change into martensite
- *Austenite start ( $A_s$ )*: temperature at which martensite begins to change in austenite
- *Austenite finish ( $A_f$ )*: the temperature at which the change in austenite is complete.

Assume that a strip of SMA begins at an initial temperature where it is completely martensite. Increasing the temperature to  $A_s$  will cause the material to start transforming in austenite. Once the temperature reaches  $A_f$ , the material is completely in austenite.

Assume that a strip of SMA begins at an initial temperature where it is completely in austenite. Decreasing the temperature to  $M_s$  causes the material to start transforming to martensite. Once the temperature is cooled to  $M_f$ , the material is completely twinned martensite.

Fig. 2.8 shows the transformation temperatures and their relation to martensite and austenite in the material.

The percentage of nickel and titanium composition plays an important role in the transformation temperatures, the transformation temperatures are sensitive to small alloy composition changes, a 1% shift in the amount of either nickel or titanium in the alloy results in a 100°C change in Af. For this reason, it is necessary to control and known the alloy composition.

In commercial Ni–Ti alloys cover an Af range from approximately 100°C in Ni50%Ti, -20°C in a Ni–Ti48.8%. Typical tolerances for Af are  $\pm 3^\circ\text{C}$  to  $\pm 5^\circ\text{C}$ , while, As is typically approximately 15°C to 20°C lower than Af, instead, Mf is about 15°C to 20°C lower than Ms.

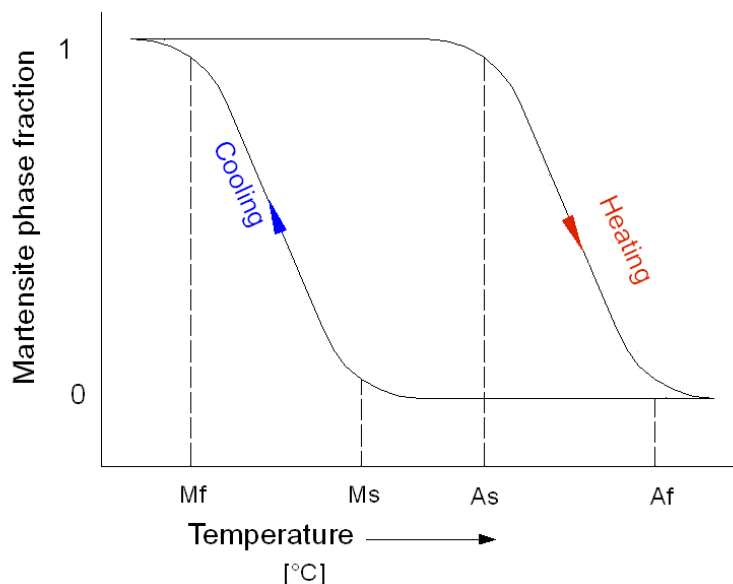


**Fig. 2.8:** Phase Transformation Temperatures of SMA material: Ms is the martensite start temperature, Mf is the martensite finish temperature, As is the austenite start temperature and Af is the austenite finish temperature.

### 2.4.1 Measuring Transformation Temperatures in Ni–Ti Alloys

There are numerous ways of determining TTRs, but there are in common use for Ni–Ti alloys to provide helpful data to product designers, three important ways: Constant Load, DSC, and Active Af [3].

**Costant Load** : it is method to apply a load to the alloy and monitor its deformation and shape recovery simultaneously with temperature as the material is cooled and heated through the transformation range. In Fig. 2.9 is shown the elongation and contraction of a shape memory wire under tensile loading as the temperature is lowered and subsequently raised. The temperature points noted are ones frequently used to describe the behavior of a particular alloy.

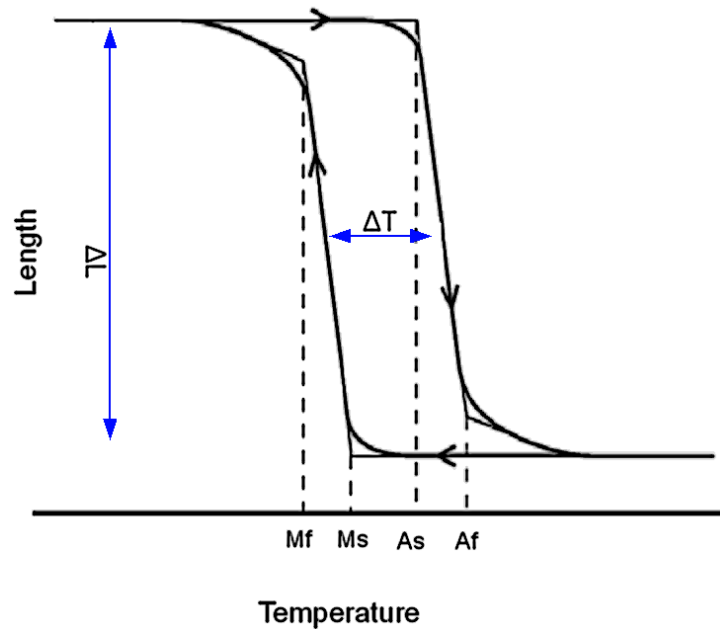


**Fig. 2.9:** Costant Load test: Specimen Length vs. Temperature of Ni-Ti, see text for details on temperature Pag. 26.

**Differential Scanning Calorimeter** : it is a method of determining the TTRs values at zero stress, but one requiring an expensive instrument, is to use a Differential Scanning Calorimeter (DSC), much better described in the next chapter. DSC is a thermoanalytical technique in which the difference in the amount of heat flow required to increase the temperature of a sample and reference are measured as a function of temperature. Both the sample and reference are maintained at

## 2.4 Temperature Transformation in Shape Memory Alloys

nearly the same temperature throughout the experiment. This DSC method yields a plot such as Fig. 2.10 by measuring the amount of heat given off or absorbed by a sample of the alloy as it is cooled or heated through its phase transformations. One important drawback to the DSC method is that tests on partially cold worked materials, such as those used to optimize superelasticity, can yield poor, inconclusive results. This same drawback also may apply to samples which have undergone a heat treatment (in the range of 400 to 600 °C) following cold working. DSC is a power method not only for determining the TTRs, but also, it allows find out if the samples exhibit the R-Phase transformation or not. Therefore, it permits to try comment on the composition and fabrication methods of the materials.

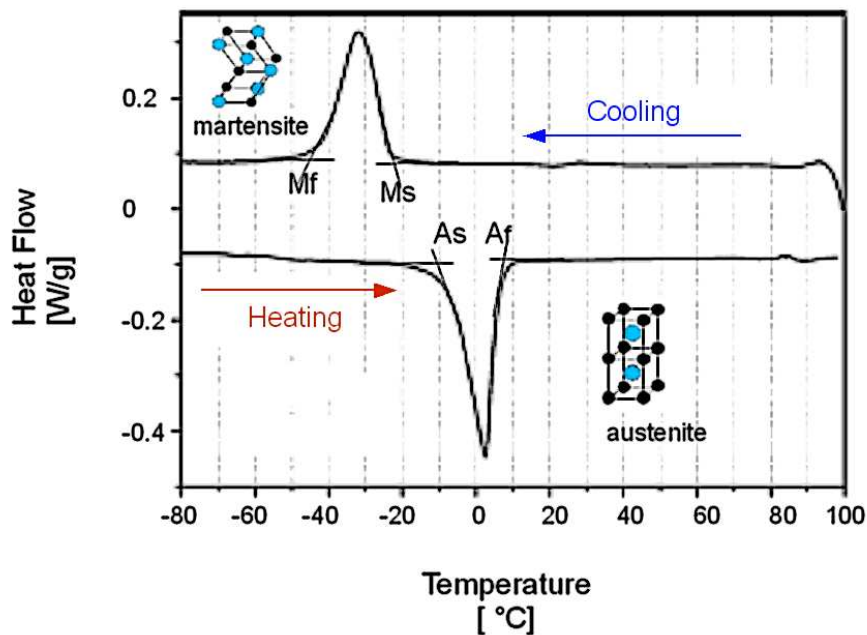


**Fig. 2.10:** Differential Scanning Calorimeter test: a typical DSC Curve for NiTi Shape Memory Alloy.

**Active  $A_f$**  : it is common namely also the Active  $A_f$  (or Functional  $A_f$ ) test. This test is conducted by merely bending a sample of the alloy, while it is below  $M_s$  and then monitoring the shape recovery while it

is heated. If a sample is gently bent into a hairpin shape by finger pressure, then warmed slowly in a stirred liquid bath while monitoring bath temperature, one can easily measure the retained bend angle at specific temperatures (plotting curves is shown in Fig. 2.11 ). This method, while not very sophisticated, will yield surprisingly accurate, repeatable results if performed carefully, and it requires very little experimental apparatus. Note that testing superelastic materials by this method requires starting at about  $-50\text{ }^{\circ}\text{C}$ . This test may be appropriate for higher temperature alloys, it is frequently used for recording the  $A_f$  of superelastic materials.

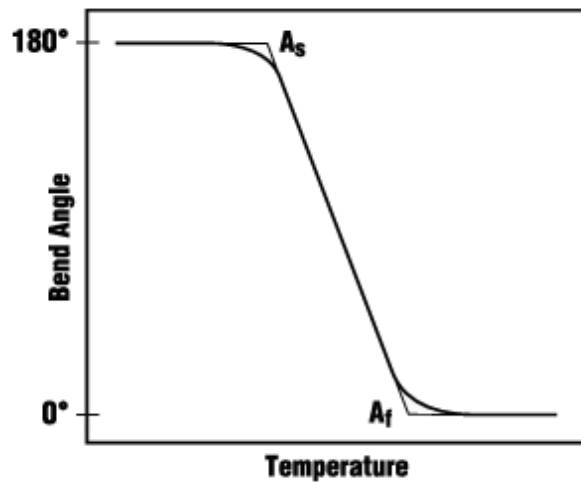
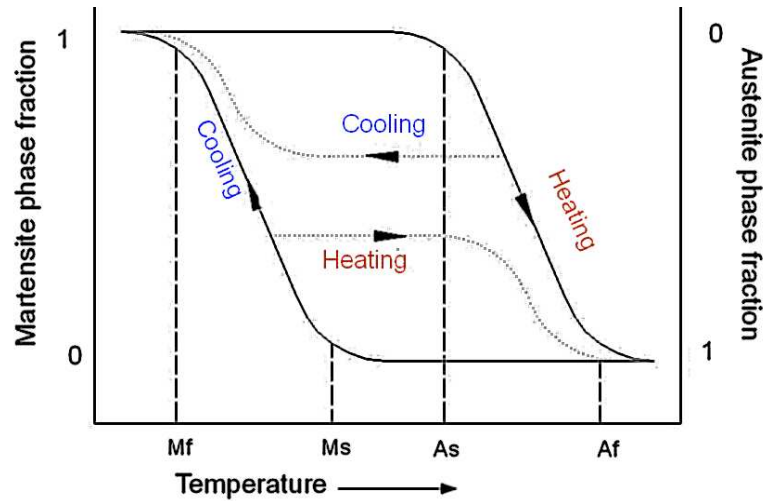


Fig. 2.11: Active Af test: a typical Active Af Test Curve for NiTi.

### 2.4.2 Hysteresis

The transformation temperature hysteresis is the difference between the temperatures at which the SMA is 50% transformed to austenite upon heating and 50% transformed to martensite upon cooling. Typical values for Ni–Ti alloys range from  $25\text{ }^{\circ}\text{C}$  to  $50\text{ }^{\circ}\text{C}$ . This hysteresis is shown in Fig. 2.12. The solid line in Fig. 2.12 is the major hysteresis path. This is the non–

linear path an SMA material follows when it cycles between the extreme temperatures,  $M_f$  and  $A_f$ .



**Fig. 2.12:** Temperature-to-phase hysteresis: solid and dotted lines represent the major and minor hysteresis loops respectively.

If the material is only partially cycled, meaning that the temperature switches between heating and cooling within the range of  $M_s$  and  $A_s$ , then a minor hysteresis loop results, as shown in Fig. 2.12 (dashed line). Note that continued cycling within the range of  $M_s$  to  $A_s$  will shift the hysteresis over a number of cycles until the alloy acquires the shape it normally has in either the fully austenite phase or the fully martensite phase. The design needs to ensure that this shift in hysteresis does not occur. Examination of the figure shows that the austenite-to-martensite transformation occurs over a lower temperature range than the martensite-to-austenite transformation.

## 2.5 Mechanical and Functional Properties of Ni–Ti Alloys

The mechanical characteristics of Ni–Ti in its two phases are interested a large number of researchers. Several experimental studies have been conducted to specify the mechanical properties of SMAs and the experimental

research developed a range for the mechanical parameters that would be expected from Ni–Ti in its austenite and martensite phases as seen above in Tab. 2.2. Since the SMA stress–strain relationship depends on temperature, the Youngs modulus also depends on temperature. Youngs modulus is the ratio of the applied stress to the resulting strain. Therefore, the mechanical behavior of a Ni–Ti alloy as a function of temperature.

At low temperature, so that in martensitic phase, the mechanical behavior of the material is characterized by large inelastic deformation after unloading that could be recovered by heating the alloy (Shape Memory Effect, SME). As the multivariant martensitic phase is deformed, a detwinning process takes place, as well as growth of certain favourably oriented martensitic variants at the expense of other variants. The mechanical loading in the martensitic phase induces reorientation of the variants and results in a large inelastic strain, which is not recovered upon unloading. At the end of the deformation, and after unloading, it is possible that only one martensitic variant remains if the end of the stress plateau is reached; otherwise, if the deformation is halted midway, the material will contain several different correspondence variants. During unloading, the detwinned martensite transforms in austenite due to its instability at temperature up than  $A_f$ , so that, a lower stress plateau, related to the reverse transformation, appears in the stress–strain–T curve (Superelastic Effect, SE), generally, without inelastic strain (see Fig. 2.13).

### 2.5.1 The Origin of Shape Memory Effect

Martensite is generally of a lower symmetry phase than Austenite (Fig. 2.7). Therefore there are several ways by which Martensite can be formed out of Austenite. However there is only one route by which the Martensite formed will revert back to Austenite.

The unique property of Ni–Ti alloys is Shape Memory Effect (SME) can be explained in a very simple manner by a 2D geometrical concept depicted. Upon cooling from Austenite, the self–accommodating variants of Martensite are formed. During the application of stress, the twin boundaries migrate

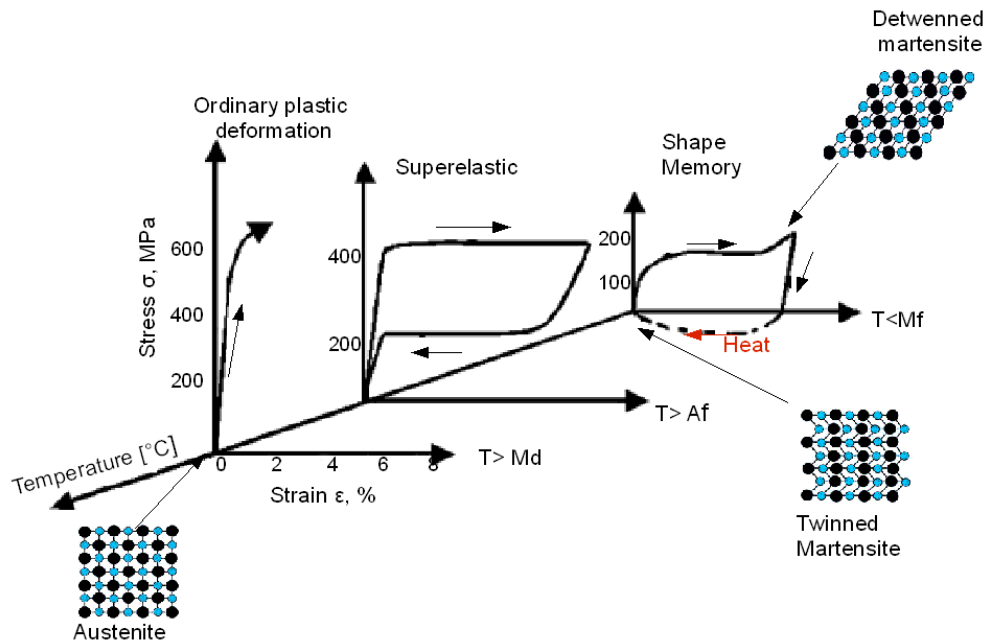


**Fig. 2.13:** Stress–Strain–Temperature: relation of SMA materials. Md is the temperature of transition among the phase pseudoelastica and that austenitica that, for the Ni–Ti alloy, it is usually above the temperature Af.

and therefore result in a biased distribution of Martensite variants. It is however important to note that no matter what the distribution of Martensite is, there is only one possible austenitic structure that these variants can revert back to. Therefore the martensitic variants must return back to the original undeformed shape after reverting back to Austenite. Therefore, the shape accommodation due to a twin boundary movement can only be supported by a low symmetrical martensitic structure, and when the more symmetric Austenite structure is returned, the twinning deformation must also disappear.

Take account of characteristic temperature (TTRs)(Fig. 2.8), there is no change in the shape of the specimen cooled from above Af to below Mf, when the specimen is deformed below Mf it remains so deformed until it is heated. The shape recovery begins at As and is completed at Af. Once the shape has recovered at Af there is no change in shape when the specimen is cooled to below Mf and the shape memory can be reactivated

only by deforming the martensitic specimen again.

Therefore, this mechanism of SME is specifically referred to the One–Way shape Memory Effect (OWSME). SME and its properties are more explain in the next subsection.

### 2.5.2 Shape Memory Effect (SME)

Shape Memory Effect (SME) is the ability to remember a predetermined shape even after several deformation. The shape changes with temperature variation are mainly attributed to martensite phase transformation. Shape Memory Effect is a phenomenon such that even though a specimen is deformed below  $A_s$ , it regains its original shape by virtue of the reverse transformation upon heating to a temperature above  $A_f$ . In particular, Ni–Ti alloys exhibits the SME when specimens are deformed below  $M_f$  or at temperature between  $M_f$  and  $A_s$ , above which the martensite becomes unstable. Depending upon the temperature range, the SME phenomenon are slightly different.

As schematically shown in Fig. 2.14, supposed, to simplify the model, to

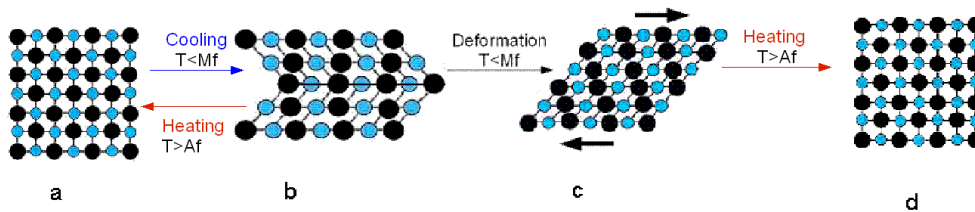


**Fig. 2.14:** a-orinal parent phase, b-self-accomodated in martensite, c-deformation in martensite(twenning and detweening), d-upon heating to a temperature above  $A_f$  (reverse transformation).

consider a single crystal in parent phase ( $T \leq M_f$ )(a). Supposed to cool the singol crystal to a temperature below  $M_f$  (b). Then, martensite are formed in a self-accomodation manner(c). Thus, if an external stress is applied, and if the stress is high enough, it will become a single variant of martensite under stress. Such a high mobility of the Twin Boundary, in which a single variant of martensite change into the twin orientation by shear. When the speciemen is heated to a temperature above  $A_f$ , reverse transformation occurs.

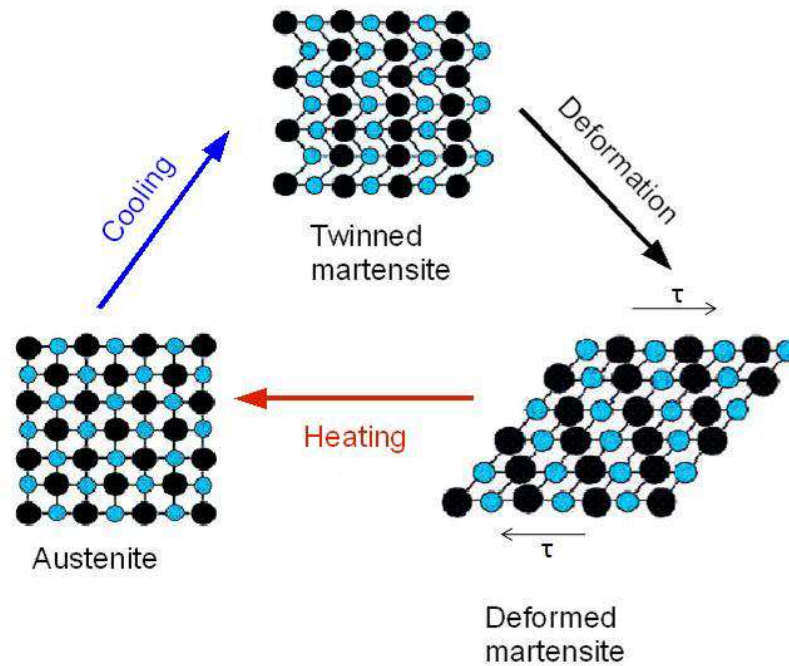


**Fig. 2.15:** Shape memory effect shown microscopically: Austenite is cooled to form twinned Martensite without undergoing a shape change, when is deformed by moving twin boundaries. Heating either state will return the originally austenitic structure and shape.

The reverse transformation induced by heating recovers the inelastic strain; since martensite variants have been reoriented by stress, the reversion to austenite produces a large transformation strain having the same amplitude but the opposite direction with the inelastic strain and the SMA returns to its original shape of the austenitic phase (d).

This is the mechanism of SME. In particular, the above described phenomenon is called One-Way Shape Memory Effect (OWSME). One Way Shape Memory Effect is an intrinsic property of SMAs, the macroscopically behavior is schematically of OWSME is explained in Fig. 2.16.

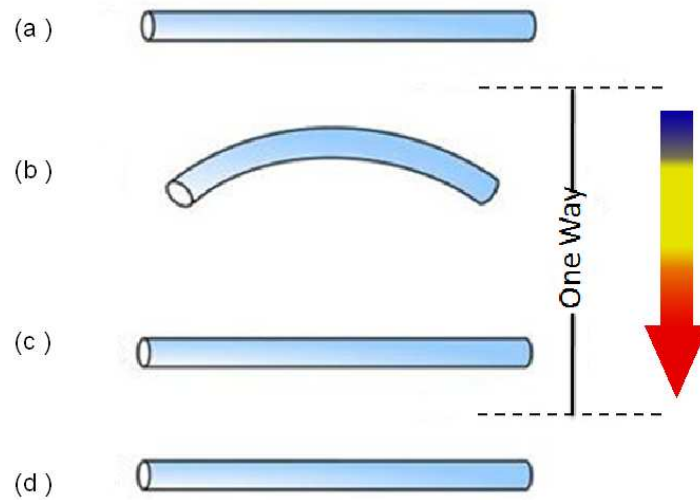


**Fig. 2.16:** Macroscopically Mechanism of One Way Shape Memory Effect: (a) Martensite, (b) Loaded and Deformed in martensite phase  $T \leq M_f$ , (c) Heated above  $T_G$  As (austenite), (d) Cooling to martensite  $T \leq M_f$ .

### Two Way Shape Memory Effect (TWSME)

The mechanism of SME describe above, only the shape of the austenitic phase is remembered. However, it is possible to remember the shape of the martensitic phase under certain condition. This behavior is a common property of SMA, it is called Two Way Shape Memory Effect (TWSME), in contrast to One Way Shape Memory Effect (OWSME) [34]. TWSME is not intrinsic property (as the OWSME) to SMA, but it can be exhibited after specific thermomechanical treatments known as *training* procedures shown in detail in Section 4.2. TWSME refers to the reversible and spontaneous shape change of materials with thermal cycling, in other words, this property permitted to SMA a spontaneous shape change on both heating and cooling. Once that the material has learned the behavior, it is possible to modify the shape of the material, in a reversible way between two different ones and without applied stress or load, only by changing of temperature across  $A_f$  and  $M_f$ . The first report of Two–Way Shape Memory Effect is due to Delay ,then to Wang and Buehler for a Ti–Ni alloy; a schematic representation of the macroscopic observed behavior is reported in Fig. 2.17

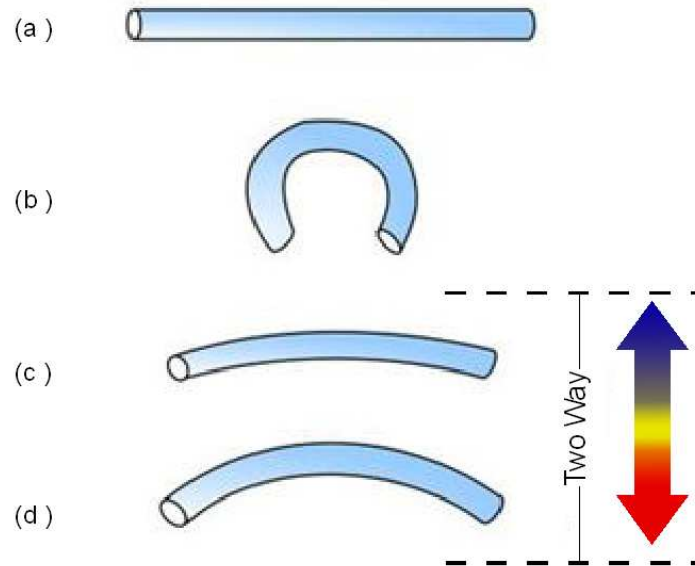


**Fig. 2.17:** Macroscopically Mechanism of Two Way Shape Memory Effect: (a) Martensite state, (b) Several deformation with an irreversible amount, (c) Heated, (d) Cooled.

At microscopic level, the reason for which a specimen remembers the shape is explanation as follows. Upon heavy deformation in martensitic phase, dislocations are introduced so as to stabilize the configuration of martensitic phase. These dislocations exist even in the parent phase after reverse martensite upon heating. In particular, there are three key microstructural forms for SMA. The first is austenite, the second is martensite described in Pag. 20. The third is a stress-biased martensite, is created either by stressing martensite below  $M_f$ , or by stressing austenite near but above  $A_f$ . This key microstructure is preferred in which becomes learned by the alloy during training process. Therefore, this structure promotes the TWSME.

### 2.5.3 Superelastic Effect (SE)

Besides the Shape Memory Effect, the SMAs also have the peculiar property known as Superelastic Effect (SE). These characteristics distinguish the SMA from the other metallurgical material.

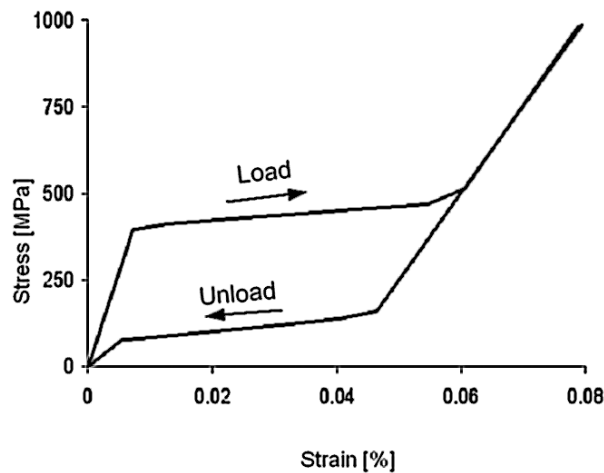


**Fig. 2.18:** Stress–Strain Curve: SE behavior of a Ni–Ti SMA, can be noticed for instance the enormous deformation reversing, that can come in some cases up to 8%.

The Superelastic Effect (SE) of Ni–Ti alloys is associated with the recovery of the deformation upon unloading. The superelastic behavior is observed during loading and unloading above  $A_f$  and is associated with stress–induced martensitic transformation and reversal to austenite upon unloading. As said until now, if the alloy is externally stressed at a temperature above  $A_f$ , it deforms transforming into a detwinned martensite, which is unstable at high temperatures, when the load is removed the SMA transforms back into austenite and the original shape of the alloy is fully recovered. The loading and unloading paths during this loading cycle do not coincide, with the unloading path being a lower stress plateau compared to the loading plateau. The Fig. 2.18 represents a typically stress–strain curve of the superelastic behavior under particular load and unload condition. In Fig. 2.19 shows a diagram representing the region of SME and SE in temperature–stress coordinates.

### Terminology

Before closing this chapter defined the terminologies Pseudoelasticity, Superelasticity and Rubber-like behavior. In fact, there is over them some confusion and they are often used indiscriminately. It is called Pseudoelas-

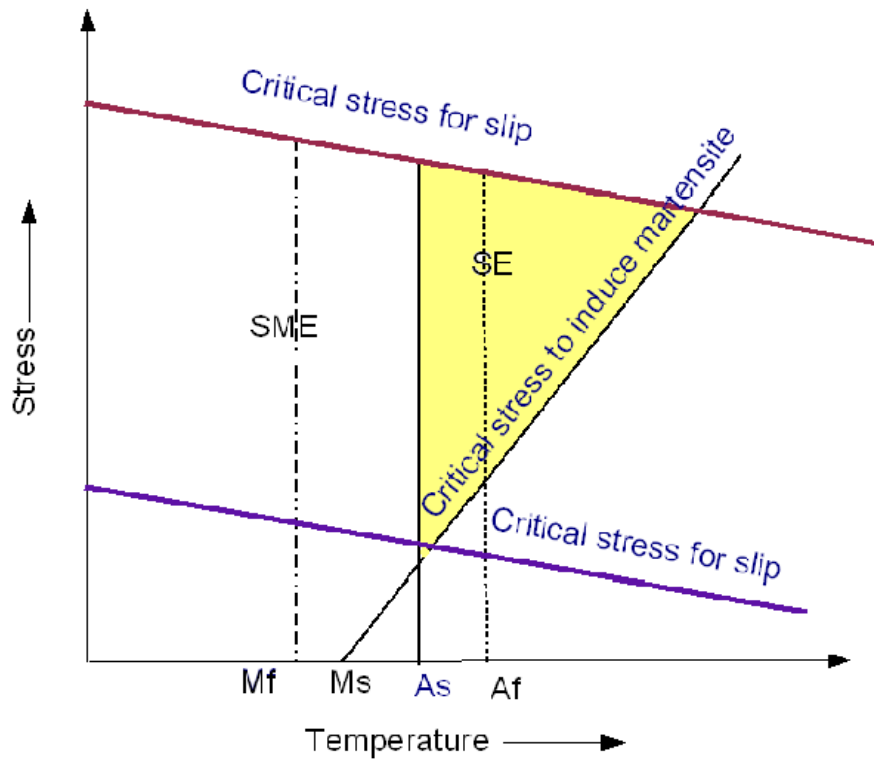


**Fig. 2.19:** Schematic Diagram representing SME and SE in temperature–stress coordinates, can be noticed the critical stress for the case of a high critical stress (red line) and the critical stress of a low critical stress (blu line).

ticity, when an apparent plastic deformation recovers just by a unloading at a constant temperature, irrespective of its origin. It is a generic term which encompasses both Superelasticity and Rubber-like behavior. When a closed loop originates from a stress-induced transformation upon loading and the reverse transformation upon unloading, it is called Superelasticity. Finally, if it occurs by the reversible movement of twin boundaries in the martensitic state, it is called Rubber-like behavior [33].

## 2.5 Mechanical and Functional Properties of Ni–Ti Alloys

---

Transformation temperatures and strains:	
Transformation temperature range	–200 - +110°C
Transformation enthalpy	0,47 - 0,62 kJ/Kg K
Transformation strains	
up to 100 cycles	up to 5%
up to 100.000 cycles	up to 3%
above 100.000 cycles	~2%
Thermal hysteresis	30 - 80°C
Physical properties:	
Melting point	~1310 °C
Density	6,45 kg/dm <sup>3</sup>
Thermal conductivity of the Martensite	~9 W/m K
Thermal conductivity of the Austensite	~18 W/m K
Electrical resistivity	50 - 110 $\mu\Omega\text{cm}$
Mechanical Properties:	
Youngs modulus of the Austenite	~70 - 80 GPa
Youngs modulus of the Martensite	~ 23 - 41 GPa
Ultimate tensile strength (cold worked condition)	up to 1.900 MPa
Ultimate tensile strength (fully annealed condition)	~ 900 MPa
Tensile strain (fully annealed)	20 - 60%
Tensile strain (cold worked)	5 - 20%

**Tab. 2.3:** Summary of Ni–Ti technical specifications: the numbers are only rough estimates covering the wide range of properties which can be achieved by either a special thermo-mechanical treatment or a slightly different chemical composition. In addition most of the properties depend strongly on the testing temperature.

## Chapter 3

# Characterization of Shape Memory Behaviour in Ni–Ti Alloys

In the previous chapter, a general description of the Ni–Ti properties are carried out in terms of mechanical and functional behaviour. In order to better understand and describe the material properties, in this chapter the results related to the experimental investigations carried out on a Ni–Ti alloys are reported. In particular, a raw Ni–Ti alloys have been characterized through thermo–mechanical treatment, so that exhibit the One Way Shape Memory behavior. Subsequently, the one way shape memory effect performances are investigate.

### 3.1 Summery of the Functional Properties

Shape memory behavior refers to a particular thermo–mechanical behavior in which small changes of some thermo–mechanical parameters, as temperature, strain and external stress. Usually, shape memory behavior refers to the recovery of a large apparently plastic deformation during heating, it is as called one way memory effect (OWSME). This property is considered that is linked with a crystallographically reversible, thermoelastic trasformation.

This reversible transformation of the austenitic phase to the martensitic phase is the basis of the following functional shape memory properties.

Below a critical temperature the sample can be deformed to an imposed shape. The apparently plastic deformation is recovered during reheating to the parent phase. Only the parent phase shape is remembered in the OWSME. Recovery stresses are generated when the OWSME is impeded. The shape recovery during heating can also occur against an opposite force, this is the work production during heating. In particular, in this dissertation, the work production during heating is called *actuator function* of shape memory alloys.

#### 3.1.1 Modelling the Shape Memory Behavior

Since, the three dimensional (stress  $\sigma$ –strain  $\epsilon$ –temperature  $T$ ) shape memory behavior is determined by the thermo–mechanical history, it is often, impossible to measure the  $\sigma - \epsilon - T$  relationship in all circumstance.

However, many mathematical models have been proposed to predict the thermo–mechanical behavior of shape memory alloys. The mathematical models are usually not very detailed, but contain a lot of coefficients which have to be determined experimentally. As results, the models are characterized by a limited fields of application.

However, the thermoelastic martensite transformation has also been the subject of many studies, in following subsection are presented one of these studies that is taking into account the contribution of defects and elastic energy.

#### 3.1.2 Thermodynamic Contribution of Defects

Consider a defect  $d_a$  with a free energy  $\Omega_d(a)$  in the parent phase structure. During transformation this defect is ‘hand down’ by the martensite structure phase. Since the crystallographic orientation of this defect depends on the orientation of the martensitic variant. So, the defect energy is indicated by  $\Omega_d(m_i)$ , where  $m_i$  is refers to  $i$ –martensitic variant. Since the transformation and the reverse transformation are diffusionless, the reverse transformation returns again in the original defect  $d_a$ . During transformation,

this defect give rise to a reversible free energy contribution  $(\Omega_d(m_i) - \Omega_d(a))$ .

Defects which are of main interest are the complex dislocation arrays generated by cycling through the transformation region. The special resulting effect is that the thermodynamic contribution of these dislocation arrays prefers the formation of the induced variants [50].

These considerations are important in the next Chapter, when will speak about the two way shape memory effect.

## 3.2 Equipments

In this chapter will discuss all the tools used as for the characterization of the material as for the analysis of the material.

- Tube Furnace and Controller : Heraeus®RO General Purpose Furnaces is suitable for thermal processes at temperatures up to 1100° C, it is including materials testing, calibrating thermocouples and chemical and physical analysis. It is equipped with heating elements on a ceramic bracing tube. The heating coils are more tightly packed at the end of the tubes to achieve an even temperature profile (Fig. 3.1). The dimension of tubular are:
  - diameter = 4,5 cm
  - tubular length = 24 cm
  
- Doric Trendicator 400a Digital Temperature Display (Fig. 3.2):
  - a) Accuracy :  $\pm 3^\circ$  to  $\pm 0.1^\circ$
  - b) Resolution :  $1^\circ/0.1^\circ/0.01^\circ$
  - c) CONFIG 400A-1-3-13-02 100-125 VA
  
- 34411A Digital Multimeter (Fig. 3.3):
  - a) 50,000 readings/s @  $4\frac{1}{2}$  – *digits* direct to PC



**Fig. 3.1:** RO tube furnace and controller.



**Fig. 3.2:** Trendicator 400a Digital Temperature Display.

- b) 1 million volatile reading memory
- c) Analog level triggering
- d) Programmable Pre/Post triggering

The multimeter are link to cromo-alumen thermocouple. Thermocouple was used to measure the temperature at different steps of current in the wire during the trials.

- Scanning Electron Microscope (SEM)(Fig. 3.4): is a type of electron microscope that images the sample surface by scanning it with a high-energy beam of electrons in a raster scan pattern. SEM fitted with BSE detector and energy dispersive microanalysis (SEM/EPMA). Sputter-

### 3.2 Equipments

---



**Fig. 3.3:** 34411A Digital Multimeter.

ing facility both with gold and carbon. Areas ranging from approximately 1 cm to 5 microns in width can be imaged in a scanning mode using conventional SEM techniques, magnification ranging from 20X to approximately 30,000X and spatial resolution of 50 to 100 nm.



**Fig. 3.4:** Scanning Electron Microscope (SEM): a typical SEM instrument, showing the electron column, sample chamber, electronics console, and visual display monitors.

- Differential Scanning Calorimetry DSC (Fig. 3.5): is widely used to examine and characterize substances, mixtures, and materials. This technique is internationally standardized under DIN 51007, DIN 53765, ISO/DIN L409 and ASTM D3418. The principle of operation is a measurement of the heat flux between the sample and reference. This is done over a well-defined area where the heat is moving. The heat flux is measured while the temperature is changing. The results are very

### 3.2 Equipments

---

important for many applications and provide valuable information for the characterization of materials. Specifications (Tab. 3.1): DSC System is completed with software and hardware including standard kits and accessories as data acquisition software to control DSC with full parameter setup and including temperature programming, atmosphere control, timed cycling etc.

Specifications	
Temperature range	$-150^{\circ}\text{C}$ up to $+700^{\circ}\text{C}$
Heating/Cooling rates	0,1 up to $50^{\circ}\text{C}/\text{min}$
Temperature accuracy	$\pm 0,2^{\circ}\text{C}$ (substance calibration)
Time constant	4...8 s
Resolution	$0,125 \mu\text{W}$
RMS Noise	$1,5 \mu\text{W}$
Data acquisition rate	0,1 s up to 3600 s / data point
Atmospheres	N <sub>2</sub> , Argon, O <sub>2</sub> etc., reducing and oxidizing
Measuring range	$\pm 2,5$ upto $\pm 250\text{mW}$
Calibrations material	included
Calibratio	recommended 6 month interval

**Tab. 3.1:** Specifications.



**Fig. 3.5:** Differential Scanning Calorimetry DSC: DSC analyzer.

- Konus microscope #5424 (Fig. 3.6): it is a microscope with a powerful 5424 stereoscopic zoom magnification ranging from 7x to 45x (up to

180x with accessories), it has a special stand in the long arm, fully adjustable ruotabilee, suitable for many specific processes.



**Fig. 3.6:** Konus microscope #5424.

### 3.3 Characterization of Ni–Ti alloy

As discussed in the Chapter 2 the Ni–Ti alloys introduce different characteristics according to the percentages of components and the thermal treatments is submitted (Pag. 10)

In this section, the results of the characterization of a equiatomic Ni–Ti alloy wires, that are in martensitic conditions at room temperature, are presented. The thermomechanical characterization was executed in terms of mechanical behaviour and Shape Memory Effect (OWSME). In this section, the results of the characterization of a equiatomic Ni–Ti alloy, that is in martensitic conditions at room temperature, are presented.

The experimental investigations were carried out using a commercial equiatomic Ni–Ti50%at. wires alloy provide by the firm Memory Metalle® ([www.memory-metalle.de](http://www.memory-metalle.de)). The Ni–Ti wires, type M ( $A_f \sim 65^\circ C$ ) and diameter equal to  $\phi = 0.49$  cm, which was produced by cold-worked and oxide free, were use for the experiments. In Tab. 3.2 is possible to see all the different types of Ni–Ti alloys in commercial and their characteristics. The

### 3.3 Characterization of Ni–Ti alloy

Effect	Types	Description
Superelastic	C	Cr-doped superelastic alloy
	N	Superelastic standard alloy
	S	Superelastic standard alloy ( $A_f \sim 0^\circ\text{C}$ )
Actuator	B	Body temperatur alloy ( $A_f \sim 35^\circ\text{C}$ )
	H	High temperature actuator alloy( $A_f \sim 95^\circ\text{C}$ )
	M	Actuator alloy with intermediate transformation temperatures( $A_f \sim 65^\circ\text{C}$ )

**Tab. 3.2:** Commercial codes based on the Ni–Ti binary system produced by the firm Memory Metalle.®

material was thermally treated, at different temperatures for different times, this treatment procedure permits to develop the OWSME in the material. The specimens were memorized various shape, and then they were testing the effectiveness of treatment (i.e. if the material after deformation recovery into shape stored during the treatment). Subsequently, it was decided to store the samples with a straight shapes, the choice of these shapes have been dictated by the mechanical tests that were subsequently made.

The NI–Ti wires were constrained on an stainless steel bar  $8 \times 2.5 \times 0,5$  cm, (see Fig.3.7) this dimensions are been dictated by the dimensions of the used tubular furnace. For the same reason, the samples straight memorized could not be extended more than 5 cm in length. The stainless steel has been select because resistant to the high temperatures and therefore reusable for all times the experiments.

The specimens were to be placed at the center of the tubular furnace, where the temperature is costant. Besides, all experiments were conducted in an unprotected environment, so it was possible to observe the presence of an oxide layer with diffrent colors for diffrent heat–tratment. As shown in Fig. 3.8, the oxidized wires are presented by SEM images. The surfaces show a typical dimple-like morphology resulting from the duration of heat–treatment [47].

The specimens were annealed at different conditions in Heraeus®furnace,

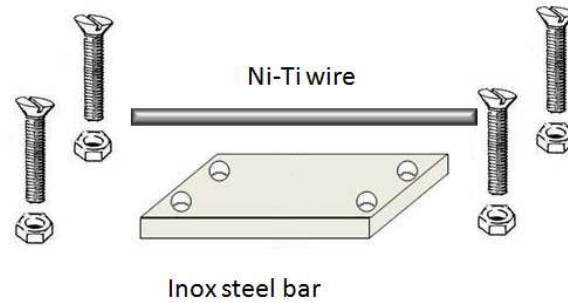


**Fig. 3.7:** Schematization Ni–Ti fixed on stainless steel bar.

and then quenched in air at room temperature for  $\sim 15$  min. The labeling of the specimens and the heat conditions are summarized in Tab.3.3.

However, for value the OWSME, the samples were cooled and deformed in martensite phase, after that they were reheated at austenite range temperature with a power supply.

This trials were repeated for every sample to value the OWSME. Every samples produced the one way shape behavior. A criterion used for the OWSME was the magnitude and the recovery rate in austenite phase. The samples produced the OWSME with better characteristics were the heat–treatment at  $610^{\circ}\text{C}$ .

After that, the measurements were performed with a Different Scanning Calorimeter (DSC). The samples for DSC analysis have been chosen in based on the same oxide colors.

### 3.4 Differential Scanning Calorimeter Analysis

Several material characterization tests were conducted to examine the properties of the produced SMAs. The first test is the Differential Scanning Calorimeter (DSC) analysis.

### 3.4 Differential Scanning Calorimeter Analysis

---

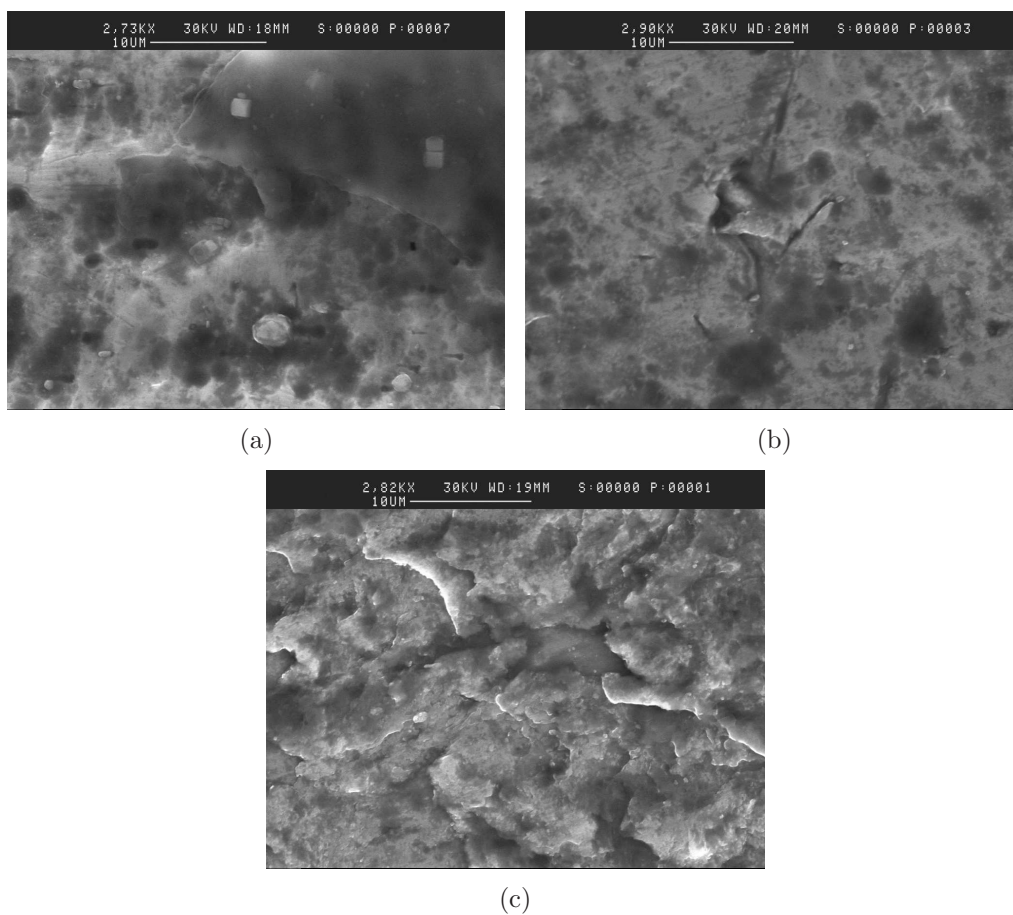


**Fig. 3.8:** Surface morphology of the wire: (a) oxidised at 490°C for 25 min, (b) oxidised at 490°C for 35 min, (c) oxidised at 490°C for 45 min.

### 3.4 Differential Scanning Calorimeter Analysis

---

Label	Temperature (°C)	Time
Sample A1	610°C	5 min
Sample A2	610°C	6 min
Sample A3	610°C	7 min
Sample A4	610°C	10 min
Sample B1	564°C	7 min
Sample B2	564°C	10 min
Sample B3	564°C	15 min
Sample B4	564°C	20 min
Sample C1	490°C	10 min
Sample C2	490°C	15 min
Sample C3	490°C	20 min
Sample C4	490°C	25 min
Sample D1	420°C	15 min
Sample D2	420°C	20 min
Sample D3	420°C	25 min
Sample D4	420°C	30 min

**Tab. 3.3:** Labeling and heat-treatment of specimens.

DSC is an instrumental technique that is used to study thermal stability, temperature and heat associated with the transformation of state and chemical reactions, in solid and liquid samples in various atmospheres. This technique is based on the detection and quantification of exothermic and endothermic phenomenon of a sample. The instrument used is formed by two resistors and two crucibles: the samples to analyzed are inserted in one, in the other one is placed the riferiment (usually it is empty). Both crucibles are connected to the thermocouples, the components are connected to a computer as shown in Fig.3.10.

The quantities of a sample required for analysis is generally a few milligrams and the speed of a heating and cooling rate depends on the ability to operational instrument used. The DSC measures the difference the heat flows in the sample and reference, while both are under the same program-controlled temperature.

### 3.4 Differential Scanning Calorimeter Analysis

---

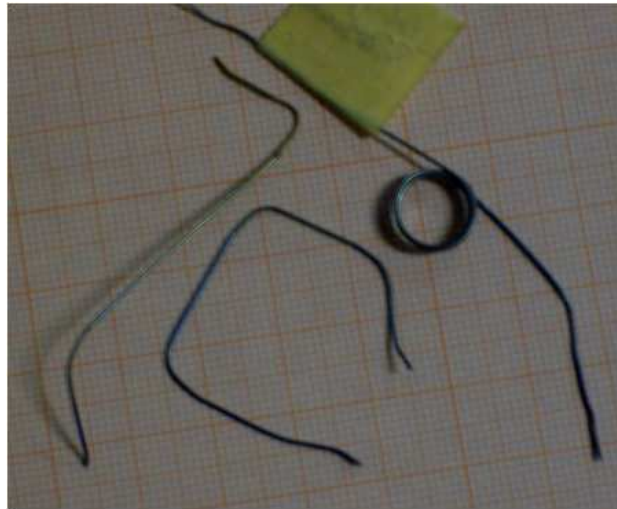


**Fig. 3.9:** Ni-Ti wires heat-treatment: the specimens were heat-treatment at different temperature to different time

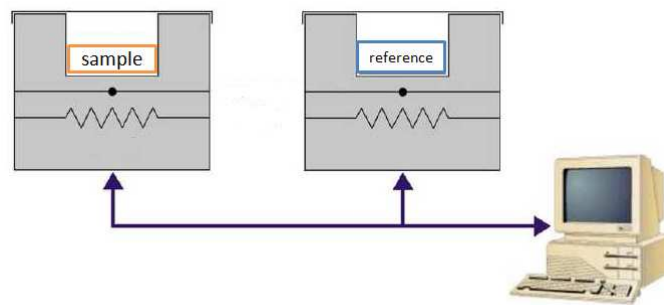


**Fig. 3.10:** Schematization of DSC analysis machine.

Temperature and heat flux measured are plotted in a diagram, where in x-axis there is the temperature and in y-axis there is heat flow. In a typical SMA diagram, it is possible measure the temperature characteristics (TTRs) as the intersection of the tangents to the inflection points of the curve, the temperatures of starting and finishing process. Beside, during cooling, it is possible note the R-phase transition, if it occurs.

### 3.4.1 Setting Conditions for Analysis

The DSC was used to analyze the thermal nature of SMA samples to compare the results with those previously reported for formed samples fabricated with different process parameters.

DSC was set to perform a temperatures program, this program consists of a heating ramp followed by a cooling ramp. Transformation temperatures of the prepared samples were determined from 0°C to 120°C using DSC equipment at the same heating and cooling rate of 5 °C/min, with cooling nitrogen system. The temperature range was chosen so that the samples exhibit a complete phase transition. Besides, the heating/ cooling rate was chosen because it considered appropriate in order to analyze the transition processes.

For each sample were carried out three thermal cycles planned, so that the samples were thermal stabilized for exhibit a complete phase transition. The DSC analysis was performed on samples annealing at different temperatures for various times. The choice of samples was done under oxide color produced. The samples analyzed are shown in the Tab.3.4, which shows the heating treatment and time of treatment

Label	Heating Temperature (°C)	Time
Sample white	cold worked	
Sample A3	610°C	7 min
Sample B2	564°C	10 min
Sample C2	490°C	20 min
Sample D3	420°C	15 min

**Tab. 3.4:** DSC samples analyzed.

## 3.5 DSC Results

First of all, the raw Ni-Ti wires alloy cold-worked were analyzed by DSC. The specimens were not subjected to heat treatment. The DSC measurements show a two-step transition on cooling and heating with very low

peaks, but close to the transition temperature given by manufacturer. In Fig. 3.11(a) is shown the raw material thermogram.

In Fig. 3.11(b) shows DSC spectra of specimens aged for various times. First of all, the thermograms show austenitic-phase transition during cooling. The DSC curves permitted to distinguishing the transition phase. In particular, on heating, the reverse transformation of the martensite,  $M \rightarrow A$ , was exhibits, on cooling, at higher heat-treatment temperature, it was possible noted the transition from austenite  $A \rightarrow R$ -phase to  $R$ -phase  $\rightarrow M$ . The DSC curves show an  $R$ -phase transformation during cooling prior to the martensitic transformation, while a reverse martensitic transformation appears during heating. The presence of  $R$ -phase is due to cold working and the oxide layer formed during the heat treatment [48]. Therefore, the presence of the  $R$ -phase is essential in the characterization of Ni-Ti alloy type M wires, as seen in literature [2].

From the DSC curves, the transformation start and finish characteristic temperatures were determined by the intersection of a base line and the tangent to a peak. The transition temperature of greater interest is  $A_f$ , given as provided by the company. In fact, as see above in Tab.3.2, type M alloys have  $A_f \sim 65^\circ\text{C}$ . As possible to see in Fig.3.11(b), each sample, after heat treatment, has  $A_f$  characteristic temperature from  $\sim 70^\circ\text{C}$  to  $\sim 75^\circ\text{C}$ . In detail, the Sample A3 and Sample D3 DSC curves were considered for the studis followed. The Sample A3 thermogram has been taken into consideration because the phase transitions were separated. The characteristic temperature of Sample A3 are (see Fig.3.12(a) ):

- $A_f \simeq 74^\circ\text{C}$
- $A_s \simeq 54^\circ\text{C}$
- $R_s \simeq 46^\circ\text{C}$
- $R_f \simeq 40^\circ\text{C}$
- $M_s \simeq 24^\circ\text{C}$
- $M_f \simeq 18^\circ\text{C}$

### 3.5 DSC Results

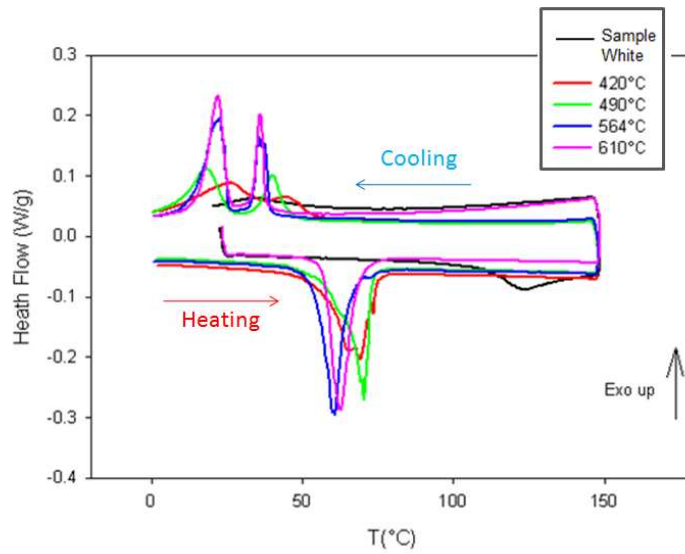
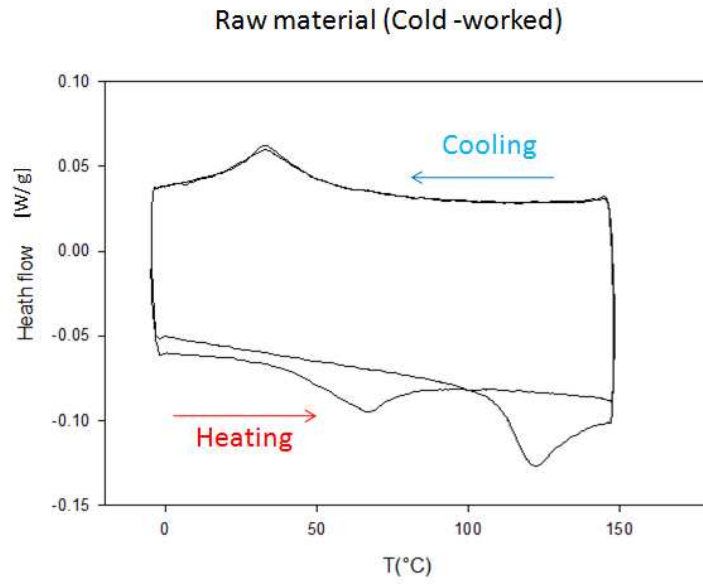


**Fig. 3.11:** DSC thermogram of a Ni-Ti alloy: (a) DSC curve of raw material cold worked, (b) DSC curves of Ni-Ti alloy wires after heat treatment.

On the contrary, in Fig.3.12(b) is shown Sample D3 DSC curve. The Sample D3 thermogram shows incomplete R-phase transformation, it passed immediately to the martensite phase transformation.

In conclusion, in DSC curve is possible to distinguish the three transitions phase when the heat treatment temperature increases. An important observation, the increase of the heat-treatment temperature, the transitions phase were better distinguished. Another observation, the time of treatment did not have correlation apparently between the transition phase and the treatment duration time.

## 3.6 X-Ray Diffraction

X-ray diffraction technique is an analytical techniques which reveal information about the crystallographic structure, chemical composition, and physical properties of materials. This technique is based on observing the scattered intensity of an X-ray beam hitting a sample. An important parameter is the wavelengths, X-rays have wavelengths on the order of angstroms, in the range of typical interatomic distances in crystalline solids. For this reason, X-ray diffraction (XRD) has provided information regarding the crystallographic structures in material. But also, it can be used to determine molecular structures. X-ray diffraction provided important evidence of atoms. XRD directed at the solid provides is the simplest way to determine the interatomic spacing. The intensity of the diffracted beams depends on the arrangement and atomic number, but also on the other parameters.

To improve the experimental behavior of aging of Ni-Ti alloy wires, after the DSC analysis, a measurements of observations by X-ray diffraction was presented. Wires of 0.49 mm diameter were observed at different heat-treatment temperatures (the same wires were studied above in DSC experimental). The X-ray measurements were made because with DSC analysis we can distinguish the transitions phase and characteristic temperature but no observe the crystallographic structure produced in the transition phase.

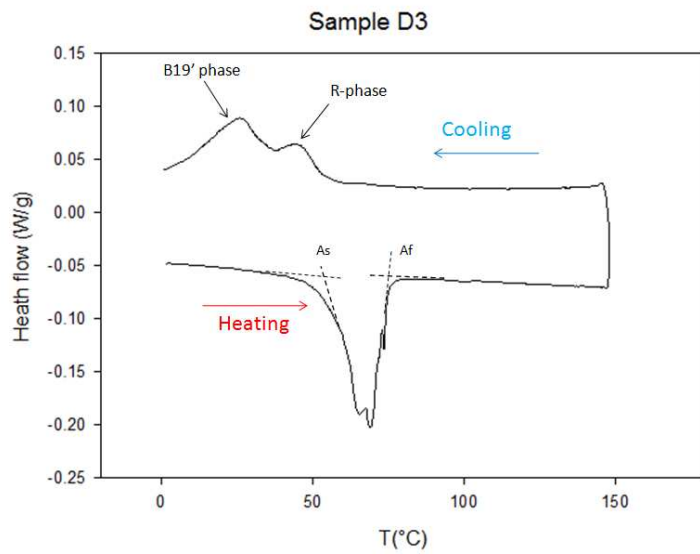
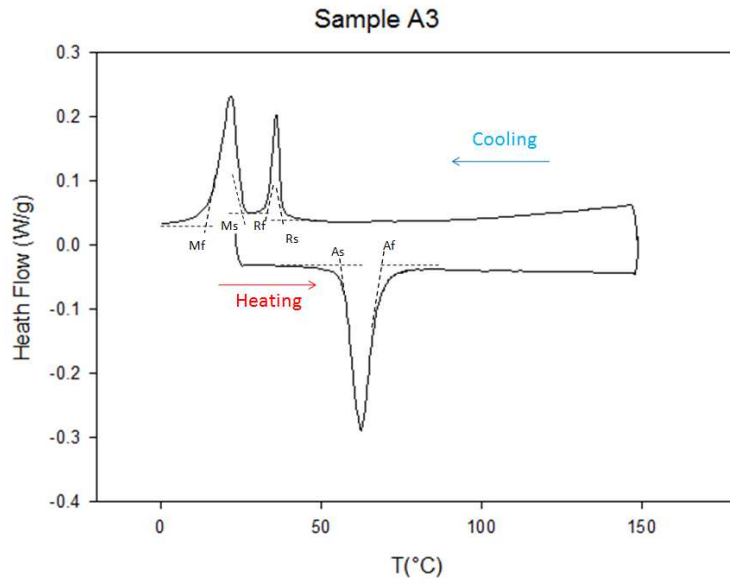


**Fig. 3.12:** DSC thermogram of a Ni–Ti alloy: (a) DSC curve of raw material cold worked, (b) DSC curves of Ni–Ti alloy wires after heat treatment.

### 3.6.1 X-ray Diffraction Analysis

In Fig.3.13 is shown the X-ray spectrum of Ni-Ti alloy wires cold-worked. As possible to observe, the material did not produce the B2 structure in austenitic phase, because the sample were not heat-treatment. In fact, the Ni-Ti wires heat-treatment at different temperature produced B2 structure in austenitic phase and B19' monoclinic structure in martensitic phase (Fig.3.14, Fig.3.15), typically of SMAs heat-treatment exhibiting the SME.

A mean observation, the B2 structure is become more evident when the heat-treatment temperature increasing (Fig.3.16). Unfortunately, the alloy oxide layer is too thin to be studied with the XRD measures used.

## 3.7 Conclusion

In this chapter, the equiatomic Ni-Ti cold-worked wires are heat-treatment at different temperature at different time, the samples were thermo-mechanical characterized. However, for value the one way shape memory effect, the samples were cooled and deformed in martensite phase, after that they were reheated at austenite range temperature with a power supply.

This trials were repeated for every sample to value the one way shape memory effect. Every samples produced the OWSME. A criterion used for the OWSME was the magnitude and the recovery rate in austenite phase. The samples produced the OWSME with better characteristics were the heat-treatment at 610°C.

After this observations a series of DSC results were studied. The samples were chose for the same oxide color exhibited. The DSC thermogrammers showed the Af coinciding to the Af supplied by Memory Metalle®. The DSC curves permetted determaning the characteristics temperature, but also was possible distinguished the transition phase. In particular, on heating, the reverse transformation of the martensite,  $M \rightarrow A$ , was exhibits, on cooling, at higher heat-treatment temperature, it was possible noted the transition from austenite  $A \rightarrow R$ -phase to  $R$ -phase  $\rightarrow M$ . The DSC results showed the

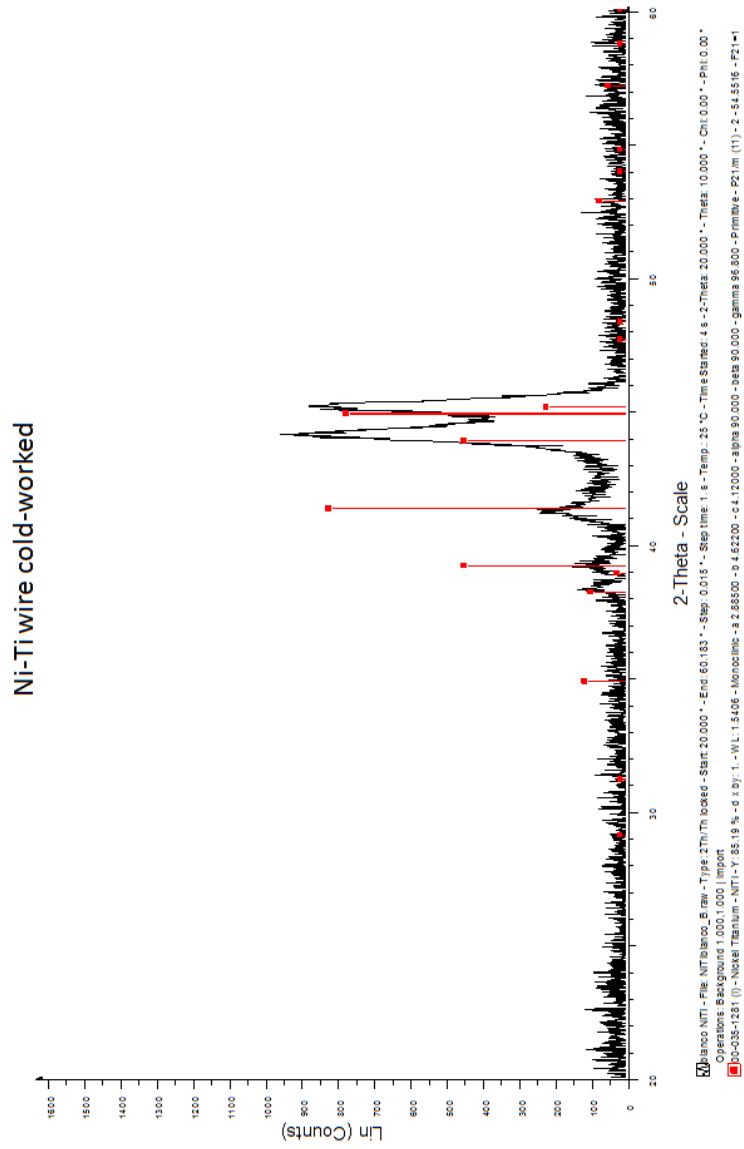


**Fig. 3.13:** XRD spectrum of a Ni-Ti alloy: XRD spectrum of raw material cold worked into the B2 structure is absent.

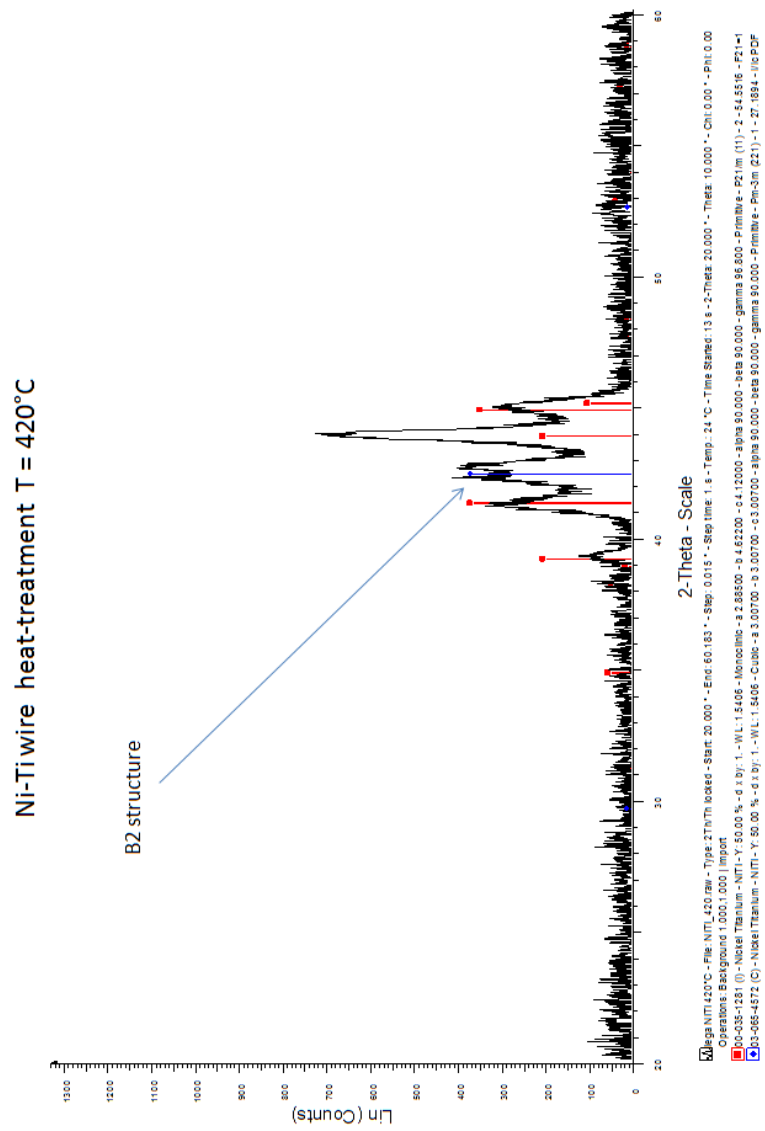


**Fig. 3.14:** XRD spectrum of a Ni-Ti alloy: XRD spectrum of Ni-Ti wires heat-treatment at 420°C into the B2 structure is appear.

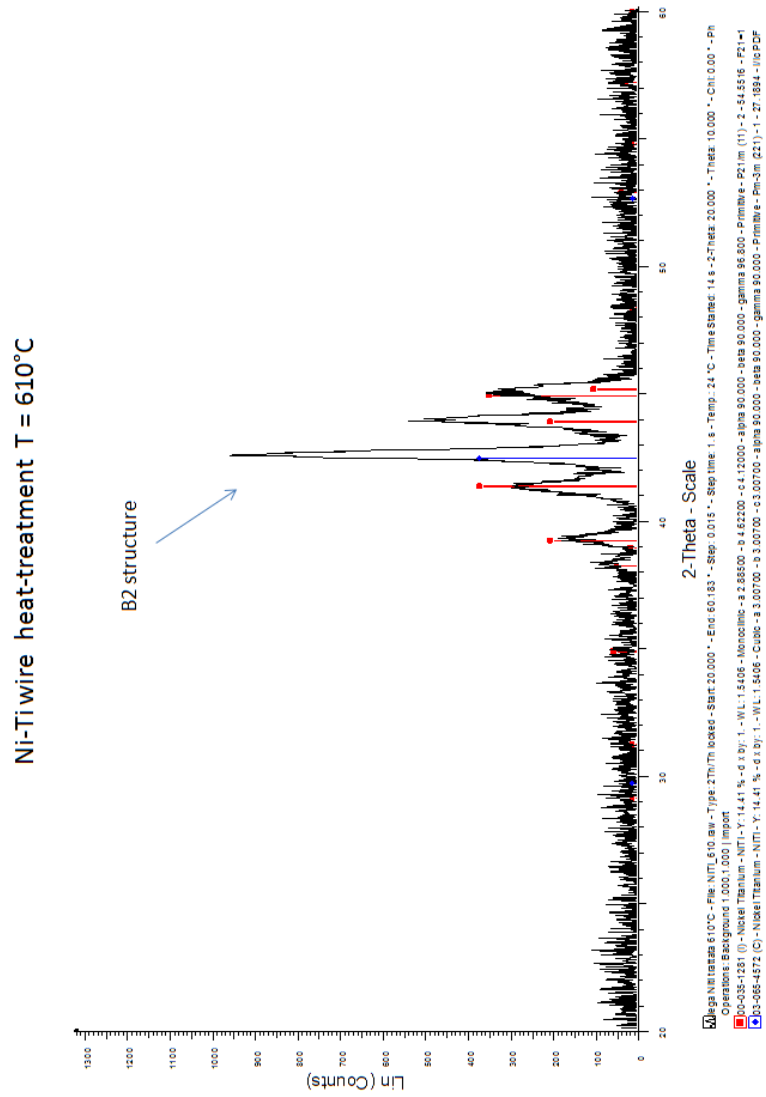


**Fig. 3.15:** XRD spectrum of a Ni-Ti alloy: XRD spectrum of Ni-Ti wires heat-treatment at 610°C into the B2 structure is more evident than the other diagram.

### 3.7 Conclusion

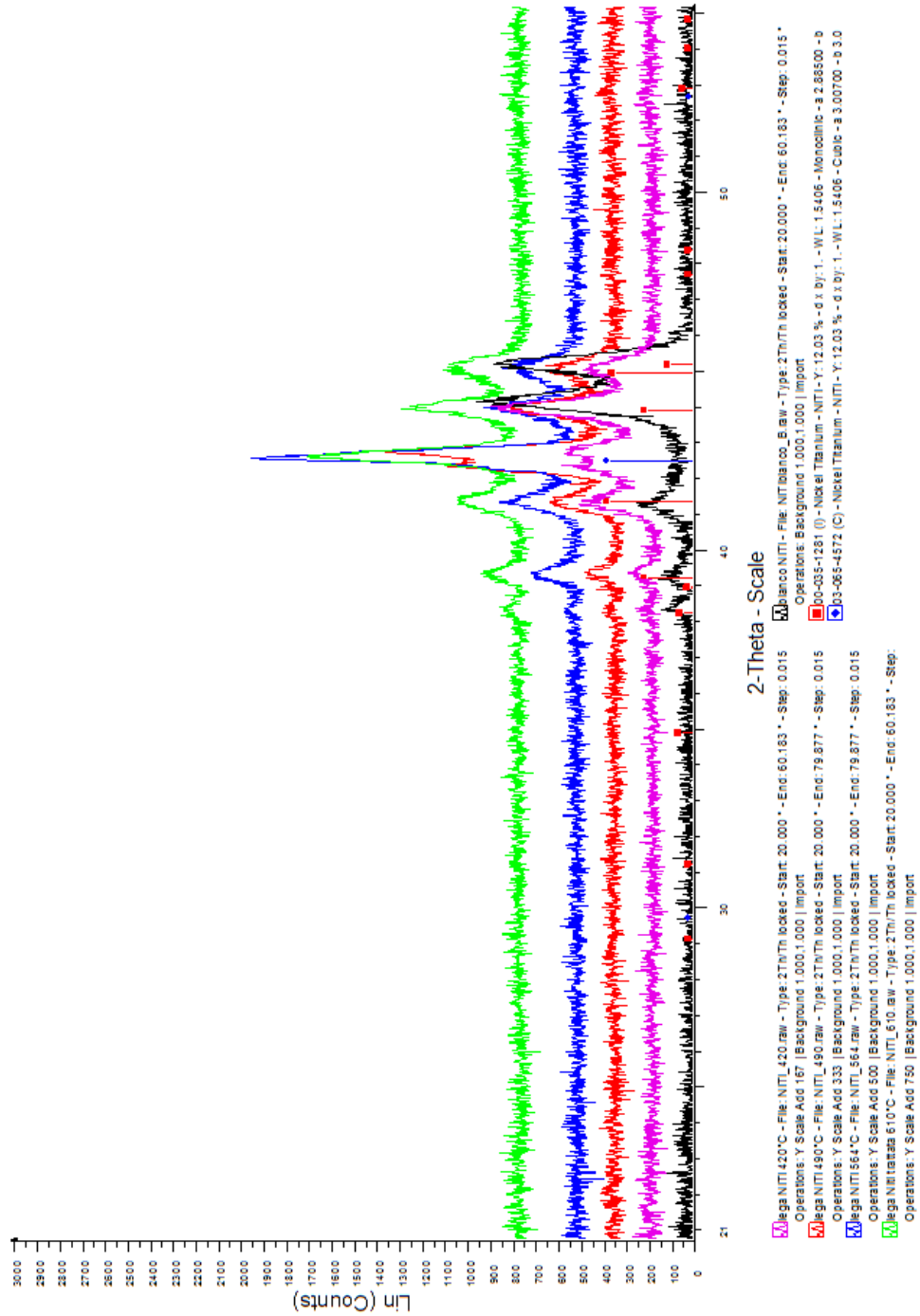


**Fig. 3.16:** XRD compared spectrum of Ni-Ti wires heat-treatment at different temperature. As noted, the B2 structure are produced in every samples without in cold-worked wires.

### 3.7 Conclusion

---

R-phase transition in every samples. But, the increase in the heat-treatment temperature, the transition phase was better distinguished. Another observation, the time of treatment did not have correlation apparently between the transition phase and the treatment duration time.

Finally, to improve the experimental behavior of aging of Ni-Ti alloy wires, after the DSC analysis, measurements of X-ray diffraction were presented. A main observation, the B2 crystallographic structure is becoming more evident when the heat-treatment temperature is increasing.

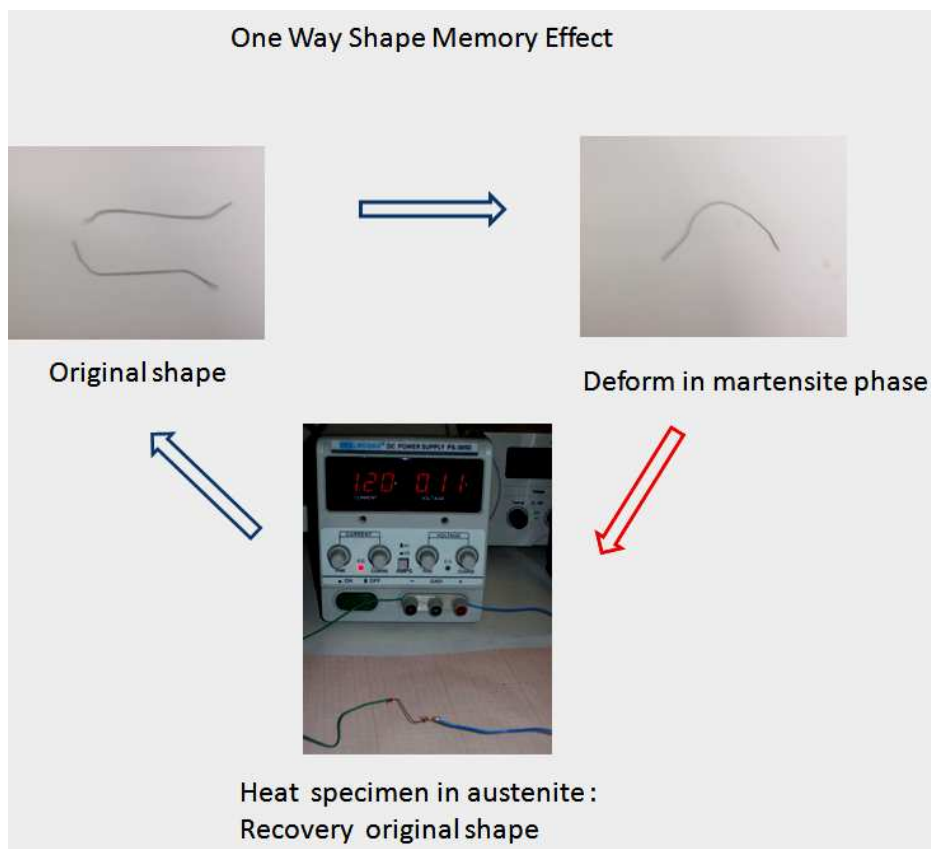


**Fig. 3.17:** Ni-Ti wires heat-treatment: the specimens were heat-treatment at different temperature to different time

## Chapter 4

# Characterization of Two Way Shape Memory Behaviour in Ni–Ti Alloys

In order to study the shape memory behaviour of the material, and to induce in it the two way shape memory effect by martensite deformation, two training procedures were carried out through the repetition of several thermo-mechanical cycles, which consist in a several deformation in martensite phase and a subsequent thermal cycle, between the temperatures  $M_f$  and  $A_f$ . The samples used are the Ni–Ti alloy wires characterized to  $610^\circ\text{C}$  for 7 minutes. In this chapter, we show the training processes for obtain two way shape memory effect and how the material was characterized by TWSME training processes.

### 4.1 Some Aspects of the Two Way Shape Memory Effect

The main difference between the two way shape memory effect (TWSME) and the other shape alloy properties is that the macroscopic shape change in TWSME is spontaneously with the temperature changing, without application of external stresses.

The origin of this spontaneous mechanism has to be attributed to some sort of anisotropy in the substructure of the austenite phase. This spontaneous shape change requires an interaction between the substructural anisotropy and the martensite formation. An important aspect is that the substructural anisotropy is not an intrinsic characteristic of the parent phase, but it is obtained after specific thermo-mechanical treatments.

These procedures are explained in the followed section (Sez. 4.2) and they are mostly known as '*training*' procedures. The exact origin and the mechanism of the TWSME obtained after training procedures can be explained by use of thermodynamic description. The origin of TWSME has to be attributed to the dislocation arrays, which are generated during training cycling. In fact, high densities of dislocation arrays with similar characteristics are produced by thermo-mechanical cycling and by thermal cycling through the transformation region. In literature, it is also found that there exists a crystallographic correspondence between these dislocation and the induced martensite variants [16],[34].

The TWSME has been ascribed to the relaxation of residual stresses by preferential martensite formation. However, inhomogeneous plastic deformation of either martensite or the austenitic phase results in an inhomogeneous residual macro stress distribution. This inhomogeneous residual macro stress distribution can result in preferential martensite formation and an accompanying shape change. This reversible shape effect is comparable with the one way memory effect, but distinct from the TWSME which is attributed to a substructural anisotropy, as in a macro scale asymmetry. The main TWSME characteristic is its magnitude. For a short time, the TWSME can be easily suppressed by applying a small opposite stress during cooling. The ability of the TWSME to act against opposite stress during cooling, can be considered an additional TWSME characteristic.

## 4.2 Two Way Shape Memory Training Processes

As mentioned in Section 2.5.2, Two Way Shape Memory Effect (TWSME) is a learned behavior for a shape memory alloys (SMAs). Under certain circumstances (Section 3.3), a SMA remembers its high temperature shape, but forgets the low temperature shape when it is deformed. Every way, it can be *trained* to remember the low temperature shape. In TWSME only temperature must be varied to affect the change in shape. SMAs that have been trained are also referred to in general literature as educated.

Most training procedures are based on the repetition of transformation cycles from the parent phase to preferentially oriented martensite. Combinations and variants of the training procedures can also be applied. In most of publications, the new aspects are listed, but no emphasis is given to the similarity with previously described procedures.

When the procedures are compared, there can be an important criterion to determine the optimum training procedure: the optimum training procedure and the optimum parameters within this procedure have to result in optimum TWSM behavior, that are a combination of maximum magnitude, reproducibility and stability of the TWSME and a minimum change of the heating shape range and of the transformation temperatures [33].

The main training procedures are described as follows.

### 4.2.1 TWSME Training by Overdeformation

The alloy is cooled below  $M_f$ , and while in the martensite state, is severely bent, to well beyond the strain limit for completely recoverable shape memory. When reheated to the parent phase, the alloy will not recover the original shape. By exceeding the shape memory strain limit, a partial loss of shape memory occurs (Fig. 4.1(a)). If the SMA is cooled again to the martensitic state, the alloy will, in a spontaneous manner, revert back toward the overdeformed shape.

This is one of the processes used in experimental training described in the next

section.

### 4.2.2 Training by Shape Memory Cycling

This procedure consists of repeatedly carrying out shape memory cycles until the two-way behavior begins. A typical first shape memory cycle consists of the component being cooled to below  $M_f$ , deformed to a level below the shape memory strain limit, and then heated to recover the original high temperature undeformed shape (Fig. 4.1(b)). After a number of such cycles (5-10 cycles) have been carried out, the component will begin to spontaneously change shape upon cooling, moving in the direction in which the component was consistently deformed during the training cycles. The amount of spontaneous shape change during cooling will be significantly less than that which was being induced in the shape memory deformation.

### 4.2.3 Training by Pseudoelastic (PE) Cycling

This method consists of repeatedly stress-inducing Martensite by loading and unloading the parent phase above the  $A_f$  temperature, but below the  $M_d$  where pseudoelastic (or superelastic) behavior is expected (Fig. 4.1(c)). As method 4.2.5, the number of training cycles required is typically on the order of 5 to 10.

### 4.2.4 Training by Combined SME/PE Training

The specimen is first deformed in the parent phase condition to stress induce a certain amount of stress biased Martensite, then cooled to below  $M_f$  while holding the induced strain in the component, then heating up to recover the original undeformed shape (Fig. 4.1(d)). When this routine is repeated a number of times, TWSM behavior will be obtained on subsequent heating and cooling.

### 4.2.5 Training by Constrained Temperature Cycling of Deformed Martensite

This is probably the most commonly used training method at present, because it is a bit easier to carry out in terms of temperature control. In this process the specimen is deformed below  $M_f$ , thus producing a stress-biased martensitic microstructure. The sample is then constrained in the deformed condition and heated to above  $A_f$  (Fig. 4.1(e)). The sample is typically cycled from below  $M_f$  to above  $A_f$  a number of times, with the sample constrained in the original deformed shape, to complete the training routine. This training method proves to be particularly effective and is relatively straightforward to carry out.

#### Limitations on the Use of Two Way Shape Memory

There are at least four important limitations on the application of TWSME:

- *Strain Limit*: There is a limit to the amount of reversible strain which can be recovered. Typically this is in the neighborhood of 2%.
- *Hysteresis*: The inherent temperature hysteresis between the heating and cooling transformations is present.
- *Low Transformation Forces on Cooling*: This means that one can push much better with the SMA on heating than on cooling. This aspect is studied in details in the next sections.
- *Upper Temperature Limit*: If too high a temperature is used during training then the memory may be most due to annealing, this phenomenon is namely in literature 'amnesia'.

## 4.3 Degradation of the Shape Memory Effect

It has been found that the global degradation behavior is influenced by a various combination of internal and external parameters. In particular, the

### 4.3 Degradation of the Shape Memory Effect

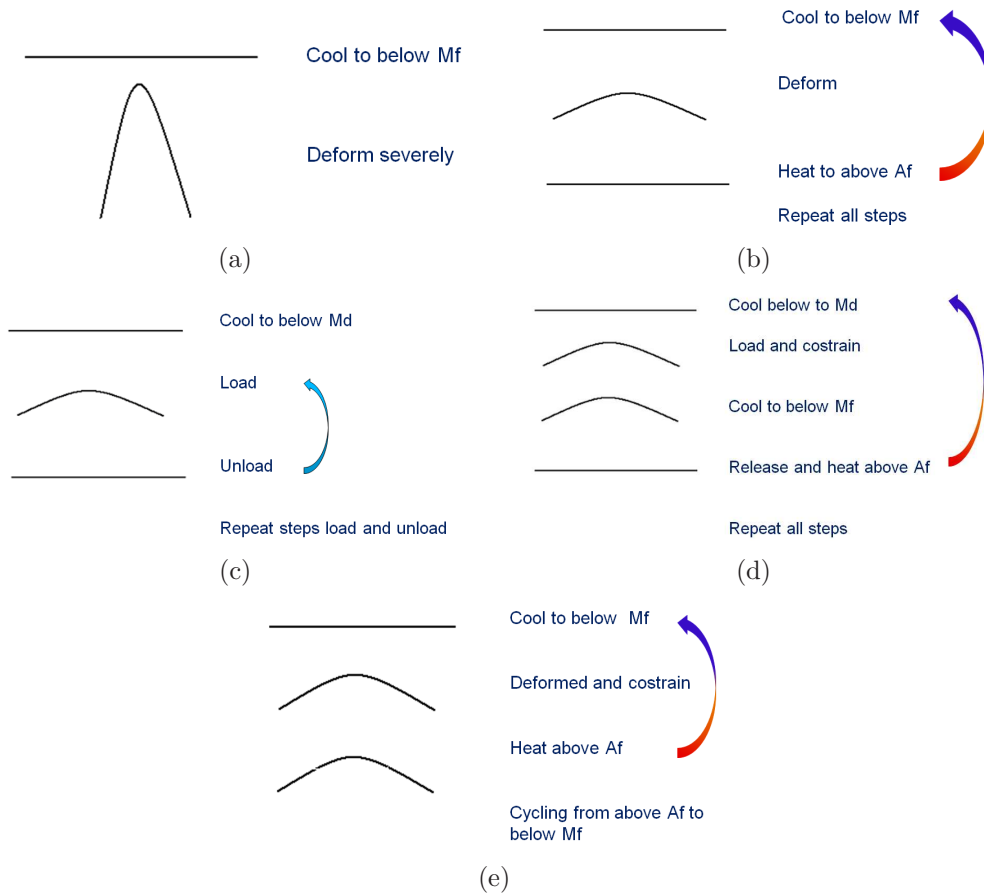


**Fig. 4.1:** Different Training Procedures that can be used to produce TWSME: (a) over deformation while in the low temperature martensitic condition, (b) repetitive shape memory cycling, (c) repetitive pseudoelastic cycling, (d) so called combined shape memory plus pseudoelastic cycling, (e) costained temperature cycling of deformed martensite.

internal parameters are: the alloy system, the alloy composition, the type of transformation, the lattice structure, including defects. Instead, the external parameters are: the thermomechanical treatment, the training procedure, the stress applied, the amplitude of temperature cycling.

Some observations revealed that the rate of degradation is also dependent on the amount of the initial TWSME. In fact, a high TWSME will degrade relatively faster than a small TWSME. Other influences are the method of training, or thermal treatment as explored in Ni–Ti alloys. In some studies are noted the importance of R–phase transition. In fact, when the cooling is stopped after R–phase transition, but before the martensite starts to grow, an improved lifetime is registered.

## 4.4 Experiment

The investigations have been carried out on equiatomic Ni–Ti wire specimens with  $\phi = 0.49$  mm, they are characterized by heat treatment to 610°C for 7 min in straight shapes. So, the material presented one way shape memory behavior. Then, the two-way shape memory effect was trained by deformation at the temperature of  $\sim 18^\circ\text{C}$  and introduced with stabilized stress-induced martensite. Therefore, the material was heated in austenite range temperature.

We applied two different training processes to the shape memory alloys straight shape.

### Method 1

The first training process consists to applied a deformation severely in martensite state as shown above in subsection 4.2.1. The shape memory alloy wire is cooled to below  $M_f$ . Then, it is deform severely in martensite. The wire was deformed using a cylinder of radius equal to 4 mm so that the wire takes a maximum strain of  $\sim 7\%$ , to well beyond the usual strain limit for completely recoverable shape memory as see in Tab.2.3. To obtain such

#### 4.4 Experiment

---

a strain was used the following equation:

$$\varepsilon_{max} = \frac{\frac{Sp}{2} \times \pi}{Ld} \approx 7\% \quad (4.1)$$

where  $Sp$  is the diameter wire(0,49mm),  $Ld$  is the wire length,  $\varepsilon_{max}$  is the maximum strain. By (4.1) was possible to derive the radius of the cylinder used as shown in Fig.4.2. After the deformation, the wire was heated to the

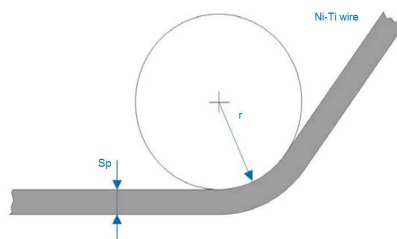


**Fig. 4.2:** Schematization of the wire profile:  $r$  is the radius of curvature .

parent phase range with a power supply. The necessary current to bring the wire in austenitic phase was measured by a type K thermocouple connected to a multimeter. The current used was  $\simeq 1,2$  A. After a number of 10 cycles, the specimen began to spontaneously change shape upon cooling, moving in the direction in which the component was consistently deformed during the training cycles as schematically illustrated in Fig.4.3(a).

With this procedure, the wire exhibits two way shape behavior: straight shape in austenite phase and a curvilinear shape in martensite phase as shown in Fig.4.3(b). The wire was reheated with a 1,2 A current and then cooled at room temperature.

#### Method 2

The second procedure used to two way shape memory behavior was described in subsection 4.2.5.

The Ni-Ti wire was cooled below  $M_f$ , the end of the wire was fixed to a joint. Then, the wire was deformed and constrained in a martensite shape by a pole, thus producing a stress-biased martensitic microstructure. The sample

#### 4.4 Experiment

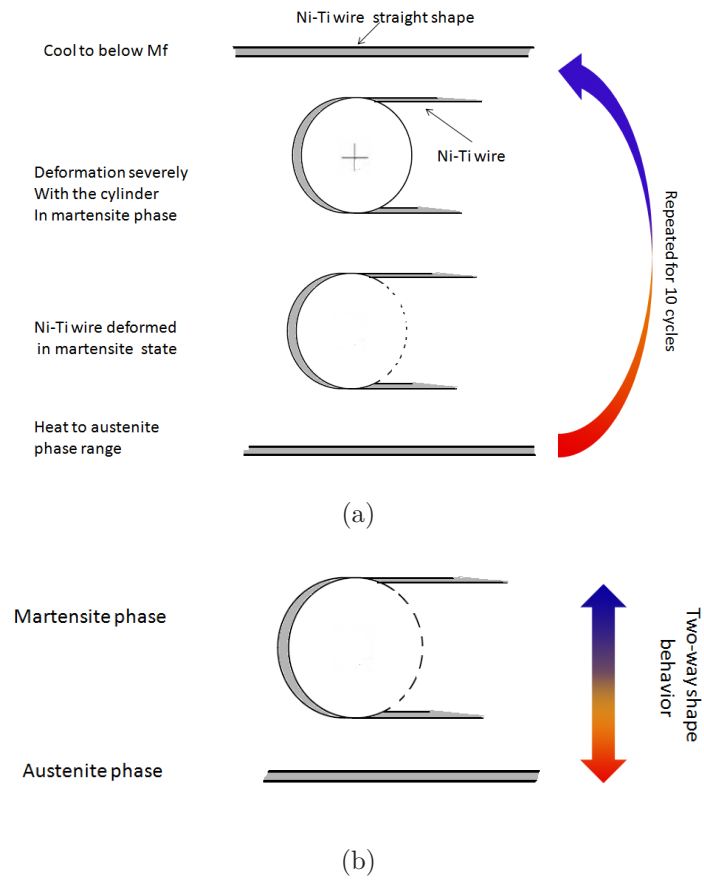


**Fig. 4.3:** (a) Schematization of procedure used to obtain TWSME: the wire straight shape is cooled below  $M_f$ , in martensite state was deformed by the cylinder and then was heated in austenite state. (b) two shape memory behavior: curvilinear shape in martensite state at room temperature, straight shape in austenite phase above  $A_s$  characteristic temperature.

in the deformed and constrained condition was heated to above  $\sim 40^\circ\text{C}$   $A_f$ . The necessary current was to equal 1,7 A. The current is greater than used in the previous method because the wire is constrained. In fact, the Ni-Ti wire requires more heat to return to the straight shape given in austenite phase due to the pole. After 20 number cycles, the specimen learned a straight shape in austenite phase and a curvilinear shape in martensite phase. In Fig.4.4 shows a schematization of used produre.

## 4.5 Results and Discussion

In this section, the results of the TWSME characterization of a Ni–Ti alloy wires, that is in martensitic conditions at room temperature, are presented. The shape memory behaviour was analyzed under training cycles executed by induce deformations in the martensitic structure. These training procedures permitted to develop the TWSME in the material and to evaluate the material deformation behaviour during repeated thermomechanical cycles executed at fixed training deformation and temperatures. But, the first observation was both methods used allow the material to learn the two way shape behavior. All samples were have undergone one of training procedures to perform the two-way memory

The experimental evidence of the TWSME, developed after the deformation, is indicative of the establishment of an internal stress field in the direction of the deformed martensite. The reverse transformation of the deformed martensite, which involves a shape change in the opposite direction to the original deformation, is resisted by this internal stress field, that, instead, guides the formation of a oriented-accommodating variant structures during the martensitic transformation, generating the TWSME of the material [34],[31], [16].

In detail, in this section, the two way shape behavior of the wires trained with Method 1 and Method 2 were compared. From previous experimental have produced the threads Ni–Ti TWSM alloy wires. The Ni–Ti wires have been conducted the experiments from which were drawn interesting comments on the methods used. In the first instance, we can observe that the learning training cycles in Method 1 are less than Method 2. Furthermore, even at cycle number 5, the material exhibits two way shape behavior in method 1. Instead, using method 2, the wires need at least 20 cycles to learned TWSM behavior. An interesting observation emerges from the recovery of shape. In fact, method 1 using, the wire does not recover the shape perfectly straight learned in OWSME, but recovers in shape to learn at low temperatures in martensite phase. On the contrary, the memorized wires with method 2 fully recover its shape both at low temperatures and shape

at high temperature in austenite range.

An important experimental test was to find out how many times the material exhibited the two way shape memory effect. The samples with method 1 recover the two shape after  $\sim 20$  heating/cooling cycles. After that, the Ni–Ti wires lost the two way shape memory effect. Hence, the wires behave as a one way shape memory material. At this point, the problem noted is the material recovers a one way shape which is a cross between the straight shape and curvilinear shape.

Instead, using the method 2, the Ni–Ti wires lose the TWSM behavior after  $\sim 100$  cooling/heating cycles, after that the wires behaved as one way shape material. But unlike method 1, the material recovers to its original learned shape, that is the straight shape in austenite phase.

## 4.6 Conclusions

Deformation by martensite reorientation causes a thermal stabilization effect on the reoriented martensite. This stabilization effect is attributed to variations in the internal elastic energy and irreversible energy that accompany the transformation [16]. Martensite reorientation deformation is effective in introducing a two way shape memory effect. The magnitude of the two-way memory effect induced by simple tensile deformation of martensite is comparable to the two way memory effect developed through conventional training procedures. A training procedure usually involves repeated deformation and transformation between the austenite and martensite temperature range. However, this experiment, demonstrates that simple deformation involving only the martensite is effective to introducing a two way shape memory behavior.

Two training procedures used were compared. The first method used a  $\simeq 7\%$  deformation and training cycles were 10, the second method use a smaller deformation than first method but the training cycles were 20. The recovery shape for the material trained with first methods decrease quickly with the increase cooling/heating cycles. In fact, the Ni–Ti wires lost the two way shape behavior after  $\sim 20$  heating/cooling cycles, but the wires did

not recovery the original shape in one way shape memory effect.

Unlike, the recovery shape of the Ni–Ti wires trained with the second procedure decreases slowly with the increase cooling/heating cycles. In fact, the samples lost the two way shape behavior after  $\sim 100$  heating/cooling cycles, but the wires did not recovery the original shape in one way shape memory effect. The advantage of using this procedure is that the specimens after lost the TWSM, they recovery the original shape learned by heat treatment.

We think that factors attributed to the two way shape memory effect were in relation to not only the annealing heat treatment but also the deformation degree and the training cycles. Whereas the thermal stabilization of martensite caused by the deformation may be attributed to variations in the internal elastic and irreversible energies based on thermodynamic considerations, the actual mechanisms as to how these energies have been changed by the deformation are yet to be established.

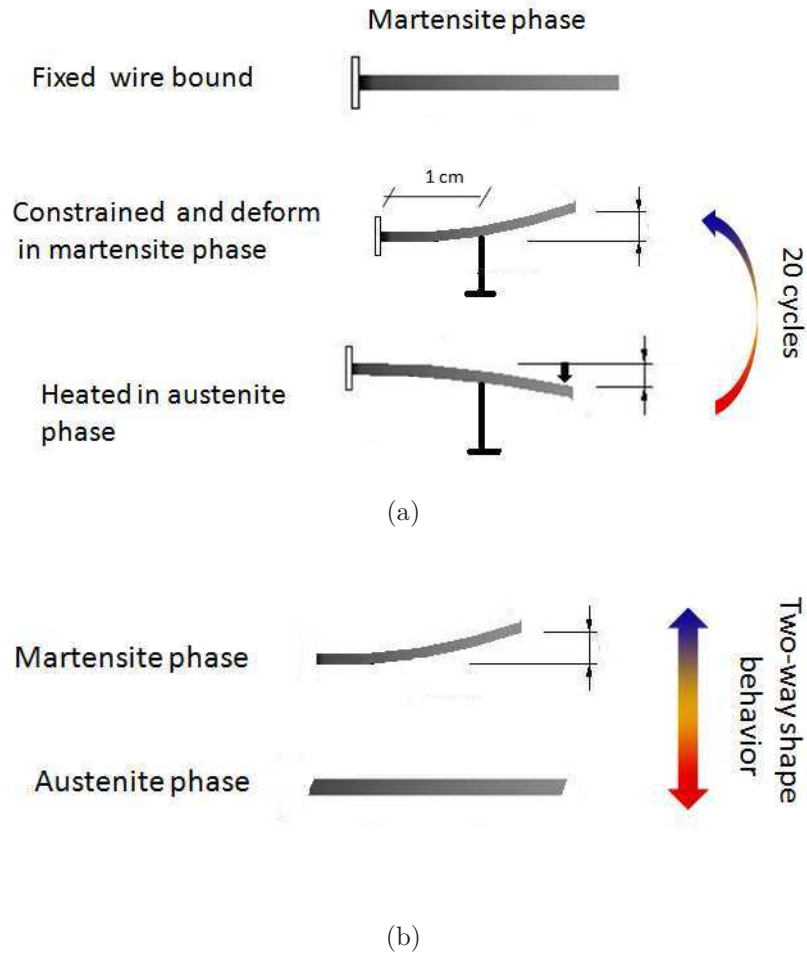


**Fig. 4.4:** (a) Schematization of second procedure used to obtain the TWSME: the wire straight shape is cooled below  $M_f$ , in martensite state was deformed and constrained, then was heated in austenite state. (b) two shape memory behavior: curvilinear shape in martensite state at room temperature, straight shape in austenite phase above  $A_s$  characteristic temperature.

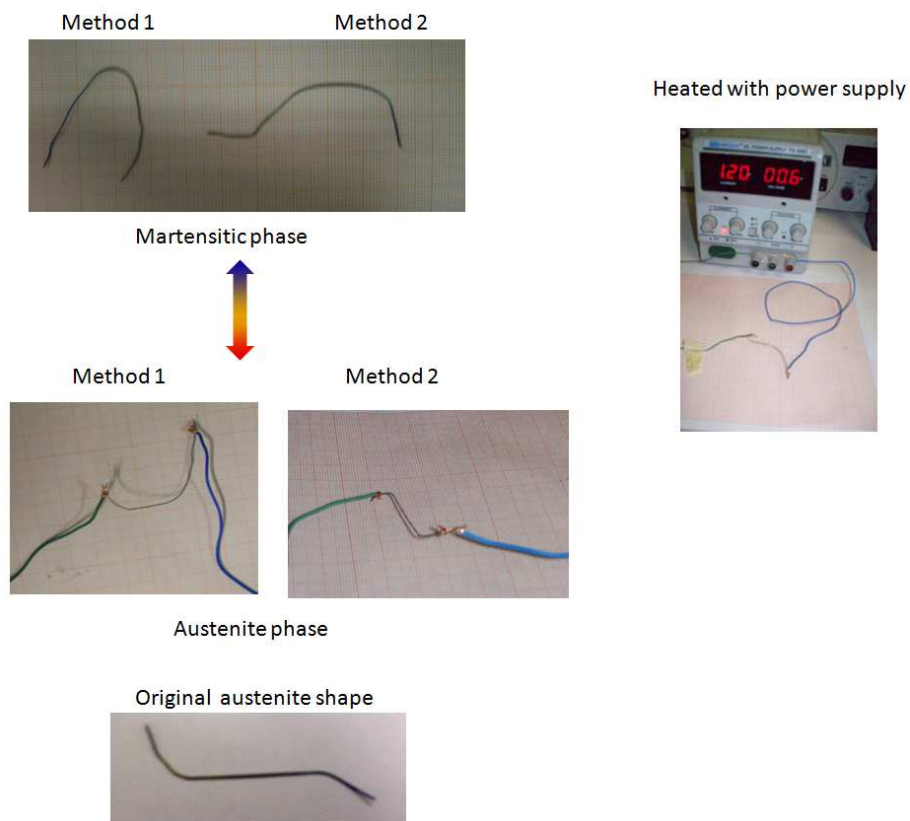


**Fig. 4.5:** Comparison the TWSME obtain with two different training procedures: shapes in martensite phase are obtained with method 1 and method 2 training procedure, the specimens are heated and in austenite phase the recovery shapes are different between the two methods to the original shape (straigh austenitic shape in OWSME).

## Chapter 5

# Conclusion and Future Developements

In this dissertation, the results of the research activities carried out during the experimental period at the University of Pavia are presented. The aim of these activities regarded the interesting field of smart materials and, in particular, some aspects related to the functional behaviour of nickel–titanium (Ni–Ti) Shape Memory Alloys (SMAs).

The research regarded different aspects concerning equiatomic Nickel–Titanium Shape Memory Alloys (SMAs). An experimental study about mechanical and functional properties of a Ni–Ti was presented in this dissertation. The present study aims to provide a more comprehensive and fondamental link between structural and various behavioral changes in Ni–Ti in response to heat treatment. This dissertation develop a more precise study on the thermo-mechanical characterization of near equiatomic Ni–Ti wires to understand the mechanism and to value the performance in One Way Shape Memory Effect and Two Way Shape Memory Effect. In particular, the deformation mechanisms involved in the material stress-strain behaviour during thermo–mechanical cycling (training procedure) was investigated.

Therefore, a general description of the Ni–Ti properties are carried out in terms of mechanical and functional behaviour. In order to better understand and describe the material properties, the results related to the experimental

investigations carried out on a Ni–Ti alloys are presented. In particular, a raw Ni–Ti wire alloys cold–worked type M have been characterized through thermo–mechanical treatment, so that exhibit a One Way Shape Memory behavior.

Subsequently, the OWSME performances are investigate, and Differential Scanning Calorimeter results were studied. However, for testing the one way shape memory effect, the samples were cooled and deformed in martensite phase, after that they were reheated at austenite range temperature with a power supply. At this point, the material exhibits the OWSME. A criterion used for the OWSME was the magnitude and the recovery rate in austenite phase. A trial procedure permitted to value the OWSME, and the conclusion was the every sample exhibit the OWSME.

Then, a series of DSC results were studied. The samples were chose for the same oxide color exhibited. The DSC thermogrammers showed the Af coinciding to the Af supplied by Memory Metalle®. The DSC curves permitted determaning the characteristics temperature and the transition phase was analized. In particular, the DSC results showed the R–phase transition in every samples. But, the increasis the heat–treatment temperature, the transitions phase were better distinguished. Another observaion, the time of treatment did not have correlation apparently between the transition phase and the treatment duration time.

After that, two training procedures were carried out through the repetition of several thermo–mechanical cycles, which consist in a several deformation in martensite phase and a subsequent thermal cycle, between the temperatures Mf and Af. The samples used are the Ni–Ti alloy wires characterized to 610°C for 7 minutes. In this chapter, we show the training processes for obtain two way shape memory effect and how the material was characterized by TWSME training processes.

A criterions to value the TWSME were the magnitude of the effect and the recovery times of the specimens.

A training procedure usually involves repeated deformation and transformation between the austenite and martensite temperature range. However, this experiment, demonstrates that simple deformation involving only the

martensite is effective to introducing a two way shape memory behavior. Two training procedures used were compared. The thermo-mechanical training induced different magnitude of the TWSME and different recovery times. In fact, the recovery shape of the Ni-Ti wires trained with the second procedure decreases slowly with the increase cooling/heating cycles, the samples lost the two way shape behavior after  $\sim 100$  heating/cooling cycles. The advantage of using this procedure is that the specimens after lost the TWSM, they recover the original shape learned by heat treatment, in accordance to literature studies.

Finally, we concluded that the factors attributed to the two way shape memory effect were in relation to not only the annealing heat treatment but also the deformation degree and the training cycles. Whereas the thermal stabilization of martensite caused by the deformation may be attributed to variations in the internal elastic and irreversible energies based on thermodynamic considerations, the actual mechanisms as to how these energies have been changed by the deformation are yet to be established.

In this dissertation was analyzed a few some aspects of Ni-Ti wires SMA. Future works should be carried to analyze the capabilities of the proposed approach in predicting the hysteretic behaviour of the material under more complex thermo-mechanical conditions, such as simultaneous variation of both stress and temperature, through specific experimental tests. In fact, the three dimensional (stress  $\sigma$ -strain  $\epsilon$ -temperature T) play an important role in shape memory behavior. Furthermore, to increase the practical usefulness of the proposed method in controlling NiTi actuators, which are usually driven by an electric current, further studies should be carried out to improve the model with the relationship current versus temperature.

Future works should be carried to analyze the R-phase transition, how this phase influences the OWSME and TWSME through specific experimental tests, in which the variables are stress  $\sigma$ -strain  $\epsilon$ -temperature T, and find out the properties and the advantages will link to this transition phase.

Future developments should be in biomedical field. In particular, Ni-Ti SMA should be large employed in the minimal-invasive surgical files, for example in endoscopical device, or tweezer for laparoscopy. The biocom-

### *Conclusion and Future Developements*

---

patibility of these alloys is one of their most important features. But, the characteristics of the TWSME properties have to study, because the several parameters play a rule in TWSME performance. In fact, the TWSME is dependent to a lot of variables, internal variables but also external variables. Future developments should be studied to analyze the internal and external variables influence the TWSM behavior, through experimental trials.

# Bibliography

- [1] *Shape Memory Applications*, chapter The Two-Way Shape Memory Effect. 1998.
- [2] *Shape memory alloys*, 2008.
- [3] E. Abel. Issues concerning the measurement of transformation temperatures of niti alloys. *Smart Mater. Struct.*, 2004.
- [4] Stöckel D. Wayman C. Duerig T., Melton K. Engineering aspects of shape memory alloys. *Butterworth-Heinemann*, 1990.
- [5] Vitchev R.G. Kumar H. Blanpain B. Van Humbeeck J. Firstov, G.S. Surface oxidation of niti shape memory alloy. *Biomaterials*, 2002.
- [6] Ortega A.M. Tyber J. Maksoundb A.El.M. Maier H.J. Liu Y. Gall K. Frick, C.P. Thermal processing of polycrystalline niti shape memory alloys. *Materials Science and Engineering A*, 2005.
- [7] Mertingerb V. Wurzela D. Hornbogena, E. Microstructure and tensile properties of two binary ni-ti alloys. *Scripta Materialia*, 2004.
- [8] Yapici G.G. Chumlyakov Y.I. Kireeva I.V. Karamana, I. Deformation twinning in difficult-to-work alloys during severe plastic deformation. *Materials Science and Engineering A*, 2005.
- [9] Schmahl W.W. Toebbens D.M. Khalil-Allafi, J. Space group and crystal structure of the r-phase in binary niti shape memory alloys. *Acta Materialia*, 2006.

- [10] Liu Y. Miyazaki S. Kim, J.I. Ageing-induced two-stage r-phase transformation in ti50.9at.%ni. *Acta Materialia*, 2004.
- [11] Puértolas J.A. Lahoz, R. Training and two-way shape memory in niti alloys: influence on thermal parameters. *Journal of alloys and compounds*, 2004.
- [12] Puértolas J.A. Lahoz, R. Training and two-way shape memory in niti alloys: influence on thermal parameters. *Journal of Alloys and Compounds*, 2004.
- [13] Huang W.M. Liu, N. Dsc study on temperature memory effect of niti shape memory alloy. *Trans. Nonferrous Met. SOC. China*, 2006.
- [14] Laeng J. Chin T.V. Tae-Hyun Namb Liu, Y. Effect of incomplete thermal cycling on the transformation behaviour of niti. *Journal of alloys and compounds*, 2006.
- [15] Liu Y. Van Humbeeck J. Liu, Y. Two-way shape memory effect developed by martensite deformation in ni-ti. *Biomaterials*, 1998.
- [16] Liu Y. Van Humbeeck J. Liu, Y. Two way shape memeory effect developed by martensite deformation in ni-ti. *Acta Metallurgica*, 1998.
- [17] Maa X. Lin C.X. Wu-Y.D. Liu, Q.S. Effect of the heat treatment on the damping characteristics of the niti shape memory alloy. *Materials Science and Engineering A*, 2006.
- [18] Van Humbeeck J. Stalmans R.-Delay L. Liu, Y. Some aspects of the properties of ni-ti shape memory alloy. *Journal of alloys and compounds*, 1997.
- [19] Van Humbeeck J. Xie Z. Liu, Y. Cyclic deformation of niti shape memory alloys. *Materials Science and Engineering A*, 1999.
- [20] Van Humbeeck J. Xie Z.-Delay L. Liu, Y. Asymmetry of stress-strain curves under tension and compression for ni-ti shape memory alloys. *Acta Materialia*, 1998.

- [21] Van Humbeeck J. Xie Z.-Delay L. Liu, Y. Deformation of shape memory alloys associated with twinned domain re-configurations. *Materials Science and Engineering A*, 1999.
- [22] Van Humbeeck J. Xie Z.-Delay L. Liu, Y. Effect of texture orientation on the martensite deformation of ni-ti shape memory alloy sheet. *Acta Materialia*, 1999.
- [23] Y. Liu. Detwinning process and its anisotropy in shape memory alloys. *Smart Materials, Proceedings of SPIE*, 2001.
- [24] Yang H. Voigt A. Liu, Y. Thermal analysis of the effect of aging on the transformation behaviour of ti-50.9at.% ni. *Materials Science and Engineering A*, 2003.
- [25] Yang H. Voigt A. Liu, Y. Thermal analysis of the effect of aging on the transformation behaviour of ti50.9at.% ni. *Materials Science and Engineering A*, 2003.
- [26] D. Mantovani. Shape memory alloys: Properties and biomedical applications. *Journal of the Minerals, Metals and Materials Society*.
- [27] H. Matsumoto. Irreversibility in transformation behavior of equiatomic nickeltitanium alloy by electrical resistivity measurement. *Journal of alloys and compounds*, 2003.
- [28] Lagoudas Dimitris C. Miller, David A. Influence of cold work and heat treatment on the shape memory effect and plastic strain development of niti. *Materials Science and Engineering A*, 2001.
- [29] Akdoğan A. Huang W.M. Nueveren, K. Evolution of transformation characteristics with heating/cooling rate in niti shape memory alloys. *Journal of materials processing technology*, 2008.
- [30] Akdoğan A. Huang W.M. Nurverena, K. Evolution of transformation characteristics with heating/cooling rate in niti shape memory alloys. *Journal of materials processing technology*, 2008.

- [31] Ren X. Otsuka, K. Recent developments in the research of shape memory alloys. *Intermetallics*, 1999.
- [32] Ren X. Otsuka, K. Physical metallurgy of ti-ni-based shape memory alloys. *Progress in Materials Science*, 2005.
- [33] Wayman C.M. Otsuka, K. *Shape memory materials*. 1998.
- [34] Hodgson D. Perkins, J. *Two way shape memory effect from Shape memory alloys*. 1998.
- [35] P.P. Poncet. Application of superelastic nitinol tubing. *MEMRY Corporation*.
- [36] S. Prof. Vasilii, Pleshanov. Ti-ni alloy with shape memory effect.
- [37] Deflorian F. Pegoretti A. D'Orazio-D. Gialanella S. Rossi, S. Chemical and mechanical treatments to improve the surface properties of shape memory niti wires. *Surface and Coatings Technology*, 2007.
- [38] Buravalla V. Mangalgi P.D. Allegavi-S. Ramamurtya U. Roy, D. Mechanical characterization of niti sma wires using a dynamic mechanical analyzer. *Materials Science and Engineering A*, 2008.
- [39] S. Russell. Nitinol melting and fabrication. In *SMST-2000 Conference proceedings*, pages 2–4, 2001.
- [40] Khmelevskaya I.Yu. Prokoshkin S.D. Inaekyan-K.E. Ipatkin R.V. Rykлина, E.P. Effects of strain aging on two-way shape memory effect in a nickeltitanium alloy for medical application. *Materials Science and Engineering A*, 2006.
- [41] T. Saburi. *Ti-Ni shape memory alloys, chap.3 of Shape memory materials*. 1998.
- [42] Zähres H. Kästner J. Wassermann-E.F. Kakeshita T. Saburi T. Somsen, Ch. Influence of thermal annealing on the martensitic transitions in niti shape memory alloys. *Materials Science and Engineering*, 1999.

- [43] A. Szod. Nitinol:shape-memory and super-elastic material in surgery. *Endoscopic Surgery service, Tel Aviv Sourasky Medical Center*, 2006.
- [44] Ganesh Kumara K. Mahesh K.K. Uchil, J. Effect of thermal cycling on r-phase stability in a niti shape memory alloy. *Materials Science and Engineering A*, 2002.
- [45] Mahesh K.K. Ganesh Kumara K. Uchil, J. Effect of thermal cycling on r-phase stability in a niti shape memory alloy. *Materials Science and Engineering A*, 2002.
- [46] Mahesh K.K. Ganesh Kumara K. Uchil, J. Electrical resistivity and strain recovery studies on the effect of thermal cycling under constant stress on r-phase in niti shape memory alloy. *Physica B*, 2002.
- [47] Joska L. Leitner J. Vojtech, D. Influence of a controlled oxidation at moderate temperatures on the surface chemistry of nitinol wire. *Applied Surface Science*, 2008.
- [48] Landa M. Lukáš P. Novák-V. Šittner, P. R-phase transformation phenomena in thermomechanically loaded niti polycrystals. *Mechanics of Materials*, 2004.
- [49] Liu Y. Wada, K. On the mechanisms of two-way memory effect and stress-assisted two-way memory effect in niti shape memory alloy. *Journal of alloys and compounds*, 2007.
- [50] Pranger W. Antretter T. Fischer-F.D. Karnthaler H.P. Waitz, T. Competing accommodation mechanisms of the martensite in nanocrystalline niti shape memory alloys. *Materials Science and Engineering A*, 2007.
- [51] Zu X.T. Wang, Z.G. Incomplete transformation induced multiple-step transformation in tini shape memory alloys. *Scripta Materialia*, 2005.
- [52] Zua X.T. Fub Y.Q. Wanga, Z.G. Study of incomplete transformations of near equiatomic tini shape memory alloys by dsc methods. *Materials Science and Engineering A*, 2005.

- [53] Jiang F. Li L. Yang-H. Liu Y. Zheng, Y. Effect of ageing treatment on the transformation behaviour of ti50.9 at.% ni alloy. *Acta Materialia*, 2007.
- [54] Cui L. Zhenga, Y. Temperature memory effect of a nickeltitanium shape memory alloy. *Applied physics letters volume*, 2004.